

Traffic Sign Extraction from Mobile LiDAR Point Cloud

Yushin Ahn, PhD Riadh Munjy, PhD Ziyuan Li



MINETA TRANSPORTATION INSTITUTE

Founded in 1991, the Mineta Transportation Institute (MTI), an organized research and training unit in partnership with the Lucas College and Graduate School of Business at San José State University (SJSU), increases mobility for all by improving the safety, efficiency, accessibility, and convenience of our nation's transportation system. Through research, education, workforce development, and technology transfer, we help create a connected world. MTI leads the [Mineta Consortium for Transportation Mobility \(MCTM\)](#) and the [Mineta Consortium for Equitable, Efficient, and Sustainable Transportation \(MCEEST\)](#) funded by the U.S. Department of Transportation, the [California State University Transportation Consortium \(CSUTC\)](#) funded by the State of California through Senate Bill I and the Climate Change and Extreme Events Training and Research (CCEETR) Program funded by the Federal Railroad Administration. MTI focuses on three primary responsibilities:

Research

MTI conducts multi-disciplinary research focused on surface transportation that contributes to effective decision making. Research areas include: active transportation; planning and policy; security and counterterrorism; sustainable transportation and land use; transit and passenger rail; transportation engineering; transportation finance; transportation technology; and workforce and labor. MTI research publications undergo expert peer review to ensure the quality of the research.

Education and Workforce Development

To ensure the efficient movement of people and products, we must prepare a new cohort of transportation professionals who are ready to lead a more diverse, inclusive, and equitable transportation industry. To help achieve this, MTI sponsors a suite of workforce development and education opportunities. The Institute supports educational programs offered by the Lucas Graduate School of Business: a Master of Science in Transportation Management, plus graduate certificates that include High-Speed and Intercity Rail Management and Transportation Security Management. These flexible programs offer live online classes so that working transportation professionals can pursue an advanced degree regardless of their location.

Information and Technology Transfer

MTI utilizes a diverse array of dissemination methods and media to ensure research results reach those responsible for managing change. These methods include publication, seminars, workshops, websites, social media, webinars, and other technology transfer mechanisms. Additionally, MTI promotes the availability of completed research to professional organizations and works to integrate the research findings into the graduate education program. MTI's extensive collection of transportation-related publications is integrated into San José State University's world-class Martin Luther King, Jr. Library.

Disclaimer

The contents of this report reflect the views of the authors, who are responsible for the facts and accuracy of the information presented herein. This document is disseminated in the interest of information exchange. MTI's research is funded, partially or entirely, by grants from the U.S. Department of Transportation, the U.S. Department of Homeland Security, the California Department of Transportation, and the California State University Office of the Chancellor, whom assume no liability for the contents or use thereof. This report does not constitute a standard specification, design standard, or regulation.

Report 24-07

Traffic Sign Extraction from Mobile LiDAR Point Cloud

Yushin Ahn, PhD

Riadh Munjy, PhD

Ziyuan Li

June 2024

A publication of the
Mineta Transportation Institute
Created by Congress in 1991

College of Business
San José State University
San José, CA 95192-0219

TECHNICAL REPORT DOCUMENTATION PAGE

1. Report No. 24-07	2. Government Accession No.	3. Recipient's Catalog No.	
4. Title and Subtitle Traffic Sign Extraction from Mobile LiDAR Point Cloud		5. Report Date June 2024	
		6. Performing Organization Code	
7. Authors Yushin Ahn, PhD Riadh Munjy, PhD Ziyuan Li		8. Performing Organization Report CA-MTI-2354	
9. Performing Organization Name and Address Mineta Transportation Institute College of Business San José State University San José, CA 95192-0219		10. Work Unit No.	
		11. Contract or Grant No. ZSB12017-SJAUX	
12. Sponsoring Agency Name and Address State of California SB1 2017/2018 Trustees of the California State University Sponsored Programs Administration 401 Golden Shore, 5 th Floor Long Beach, CA 90802		13. Type of Report and Period Covered	
		14. Sponsoring Agency Code	
15. Supplemental Notes 10.31979/mti.2024.2354			
16. Abstract <p>The extraction of traffic signs from Mobile Light Detection and Ranging (LiDAR) point cloud data has become a focal point in transportation research due to the increasing integration of LiDAR technologies. LiDAR, a remote sensing technology, captures detailed three-dimensional point cloud data, offering a comprehensive view of the surrounding environment. Mobile LiDAR systems mounted on vehicles enable efficient data collection, particularly for large-scale road networks. This study aims to develop and refine techniques for extracting traffic signs from Mobile LiDAR point cloud data, essential for enhancing road safety, navigation systems, and intelligent transportation solutions. By leveraging LiDAR technology, new possibilities for automating traffic sign recognition and mapping emerge. The research focuses on detecting traffic signs using Mobile LiDAR point cloud data, employing an intensity-based sign extraction method to identify traffic signs, traffic signals, and other retro-reflective objects. The workflow involves managing LiDAR Aerial Survey (LAS) datasets, including tasks such as merging/splitting, gridding, and detecting high-intensity features. Identified signs are visualized in Google Earth Pro, facilitating their display in Geographic Information Systems (GIS). Furthermore, the study explores point density analysis, establishing connections with potential grid resolutions for additional extraction or analysis, such as road condition assessments or crack detection.</p>			
17. Key Words Transportation, Traffic signs, MTLs, Mobile LiDAR, Point Cloud		18. Distribution Statement No restrictions. This document is available to the public through The National Technical Information Service, Springfield, VA 22161.	
19. Security Classif. (of this report) Unclassified	20. Security Classif. (of this page) Unclassified	21. No. of Pages 54	22. Price

Copyright © 2024

by **Mineta Transportation Institute**

All rights reserved.

DOI: 10.31979/mti.2024.2354

Mineta Transportation Institute
College of Business
San José State University
San José, CA 95192-0219

Tel: (408) 924-7560

Fax: (408) 924-7565

Email: mineta-institute@sjsu.edu

transweb.sjsu.edu/research/2354

ACKNOWLEDGMENTS

This research was funded by the California State University Transportation Consortium and the Fresno State Transportation Institute. The authors appreciate the editorial service and reviews they have received, as well as the assistance of FSTI and MTI administrative staff.

The authors also would like to thank the California Department of Transportation (Caltrans), District 11 Land Surveys, Ned Salman, Diego Alvarado, Angel Murillo, and Timothy Hajda for providing an MTLS data set for us to study. This research would not have been possible without the MTLS data from the Caltrans Land Surveyor team.

CONTENTS

Acknowledgments.....	vi
List of Figures	viii
List of Tables.....	x
Executive Summary	1
1. Introduction	2
2. Mobile Terrestrial Laser Scanning Data.....	4
2.1 MTLS Dataset	9
2.2 Workflow	10
3. Results and Analysis.....	19
3.1 Aerial LiDAR vs. Mobile LiDAR.....	19
3.2 Point Density on the Road Surface in Mobile LiDAR Data.....	21
3.3 Point Density on Traffic Signs	25
3.4 Traffic Sign Extraction.....	26
4. Summary and Conclusion	31
Appendix A.....	32
Appendix B	35
Bibliography.....	41
About the Authors	43

LIST OF FIGURES

Figure 1. A Photo of the Riegl VMX-1HA Scanner	5
Figure 2. Example of Traffic Signs and a Concrete Median Divider in Google Street Map (Left) and MTLS Point Cloud Data (Right)	6
Figure 3. Example of Road Marks on Google Street Map (Left) and MTLS Point Cloud Data (Right)	7
Figure 4. Example of the Road Condition on Road Marks in the Google Street Map (Left) and MTLS Point Cloud Data	7
Figure 5. Example of a Cross-Section in an MTLS Point Cloud (Upper) and a Detailed Surface Contour Representation	8
Figure 6. Example of Measuring the Dimensions of a Concrete Median Structural Barrier	8
Figure 7. Trajectory Plot of MTLS Data on Highway 76	9
Figure 8. Workflow of Traffic Sign Extraction	10
Figure 9. Illustration of Subset Rectangular Boundaries of LAS Files	11
Figure 10. Example of a Shadow Effect in the LiDAR Scan	12
Figure 11. Screenshots of A Merged Subset	12
Figure 12. Original Mobile LiDAR Subset	13
Figure 13. Intensity Map	14
Figure 14. Histogram of Point Cloud Intensity	14
Figure 15. High Intensity Rectangle Feature	15
Figure 16. Extracted Traffic Signals	18
Figure 17. Sample of Aerial LiDAR Data	19
Figure 18. Point Density Map, Number of Points	20
Figure 19. 1 Meter, Surface Map (Upper) and Intensity Map (Lower)	21

Figure 20. Density Analysis, Mobile LiDAR Data	21
Figure 21. Point Density: Number of Points Per Sq. Ft.	22
Figure 22. Resolution Map.....	23
Figure 23. Intensity Maps From MTLS Data	23
Figure 24. Point Density of Sign I	25
Figure 25. Point Density of Signs II and III	26
Figure 26. Ground Truth Signs In Subset 16	27
Figure 27. Extracted Signs, Subset 16	27
Figure 28. Display of KML Files on Google Earth Pro of Subsets 10–20	28
Figure 29. Front View of Extracted Traffic Signs and Traffic Signals in Subsets 10–20.....	28
Figure 30. Side View of Extracted Signs and Traffic Signal in Subset 10–20	29
Figure 31. Colors on Traffic Signs	30
Figure 32. 2D Hough Transformation Space	32
Figure 33. Example of Plane Detection Using Hough Transformation	33
Figure 34. Traffic LAS Visual C++ Program	34
Figure 35. Example of Manual Filtering Pre-Process.....	36
Figure 36. Example of Manual Definition of Categories	36
Figure 37. Labeled Point Cloud Data Sets in MATLAB	37
Figure 38. Trained Result Based on Our Labeled Data 1.	38
Figure 39. Trained Result Based on Our Labeled Data 2	39
Figure 40. Trained Result Based on Our Labeled Data 3	39

LIST OF TABLES

Table 1. Traffic Sign Extraction Results, Subsets 11–20.....	29
--	----

Executive Summary

The extraction of traffic signs from Mobile Light Detection and Ranging (LiDAR) point cloud data has become a pivotal focus in research, driven by the growing integration of LiDAR technologies in transportation applications. LiDAR, a remote sensing technology, captures highly detailed three-dimensional point cloud data, offering a comprehensive representation of the surrounding environment. The advantage of efficient data collection for large-scale road networks is particularly evident with Mobile LiDAR systems mounted on vehicles.

This study is centered on developing and refining techniques for extracting traffic signs from Mobile LiDAR point cloud data. The precise detection and localization of traffic signs are crucial for enhancing road safety, navigation systems, and intelligent transportation solutions. The incorporation of LiDAR technology in this context opens up new possibilities for automating the recognition and mapping of traffic signs.

The research specifically delves into the detection of traffic signs using Mobile LiDAR point cloud data. The intensity-based sign extraction method efficiently identifies traffic signs, traffic signals, and other retro-reflective objects, providing valuable insights for transportation asset management. The workflow begins with the management of the LiDAR Aerial Survey (LAS) dataset, encompassing tasks such as merging/splitting, gridding, and detecting high-intensity features. Subsequently, the identified signs are placed in Google Earth Pro, enabling their seamless display in Geographic Information Systems (GIS).

Furthermore, the study explores point density analysis, establishing a connection with potential grid resolutions for additional extraction or analysis, such as road condition assessments or crack detection.

Additionally, the research delves into the investigation of deep learning point classification and Hough transformation plane detection. The outcomes and limitations of these approaches are comprehensively summarized.

1. Introduction

Various roadside infrastructures along state or local roads are routinely managed by a state's Department of Transportation (DOTs). Challenges exist in collecting the data and maintaining the inventory. Recently, state DOTs have been adapting laser scanning technology, which digitally stores roadside information in the form of a massive number of three-dimensional points. Laser scanning refers to technology that computes three-dimensional coordinates using laser-based distance and direction measurements.

Traffic sign extraction from Mobile Light Detection and Ranging (LiDAR) point cloud data has emerged as a crucial area of research, driven by the increasing adoption of LiDAR technologies in transportation applications. LiDAR, a remote sensing technology, captures highly detailed three-dimensional point cloud data, providing a comprehensive representation of the surrounding environment, providing insights into the condition, placement, and visibility of traffic signs.

Mobile LiDAR systems mounted on vehicles offer the advantage of efficient data collection for large-scale road networks (Williams et al., 2013; Gargoum & El-Basyouny, 2019). The contribution of MTLs in management of traffic signs includes: (1) Detection and Inventory, (2) Condition Assessment, (3) Visibility Analysis, (4) Geospatial Integration, (5) Safety Enhancement, (6) Automation and Efficiency, etc.

This study focuses on the development and refinement of techniques for the extraction of traffic signs from Mobile LiDAR point cloud data. Accurate detection and localization of traffic signs play a pivotal role in enhancing road safety, navigation systems, and intelligent transportation solutions. The utilization of LiDAR technology in this context opens up new possibilities for automating the process of traffic sign recognition and mapping.

Several studies have demonstrated the potential of LiDAR for road infrastructure analysis and object detection (Ghallabi et al., 2019; Zhang et al., 2019; Wu et al., 2015; Javanmardi et al., 2019). Our research builds upon these foundations, aiming to address the specific challenges related to traffic sign extraction. The three-dimensional nature of LiDAR point clouds provides valuable depth information, enabling a more nuanced analysis of a road's environment (Yen et al., 2011).

In this study, we investigated the use of point cloud data in road-side feature extraction. The main objectives were: laying out the workflow to handle LAS files, merging and splitting files, gridding the point cloud, creating an intensity map, and finally detecting traffic signs and locating them in the Geographic Information System. In the course of the investigation, we also tested plane extraction using a 2D Hough transformation and deep learning point classification.

In section II, we introduce a general specification for Mobile Terrestrial Laser Scanning (MTLS) data and the proposed workflow. In section III, Results and Analysis, we demonstrate the point

density and optimal gridding resolution analysis on aerial laser scanning data, on the ground detection, and on traffic signs from MTLs, along with the traffic sign extraction results. In Appendices A and B, we summarize the plane extraction method and a deep learning classification test.

2. Mobile Terrestrial Laser Scanning Data

Mobile Terrestrial Laser Scanning (MTLS) data refers to three-dimensional point cloud information obtained through the use of terrestrial laser scanners mounted on mobile platforms, such as vehicles, together with other sensors. Terrestrial laser scanning involves the emission of laser beams toward surfaces, with the reflected signals captured by sensors to create precise, high-resolution, 3D representations of the surrounding environment.

In the context of mobile applications, MTLS employs laser scanners mounted on moving platforms, typically vehicles, to rapidly collect detailed point cloud data along roadways, infrastructure, or other surfaces. The mobile setup allows for efficient and comprehensive data acquisition over large areas, making MTLS particularly useful for mapping and analyzing transportation networks, urban environments, and infrastructure assets.

MTLS systems are often integrated with other sensors such as cameras, Global Navigation Satellite System (GNSS) receivers, and Inertial Measurement Units (IMUs) to enhance the accuracy and richness of the collected data. This integrated approach enables the simultaneous acquisition of geometric, visual, and positional information, making MTLS data valuable for applications such as road asset management, urban planning, and environmental monitoring.

Figure 1. A Photo of the Rieggl VMX-1HA Scanner



Figure 1 shows a photo of an MTLS system, a VMX-1HA scanner. This scanner measures 1.1 million points per second, with the point density near the scanner reaching up to 7,000 points/m². The average point density on the road is more than 4,000 points/m² (Yu, 2014). This point density translates to around 400 points/ft².

In typical MTLS systems, four components are integrated into the system to obtain accurate geo-referenced point cloud data:

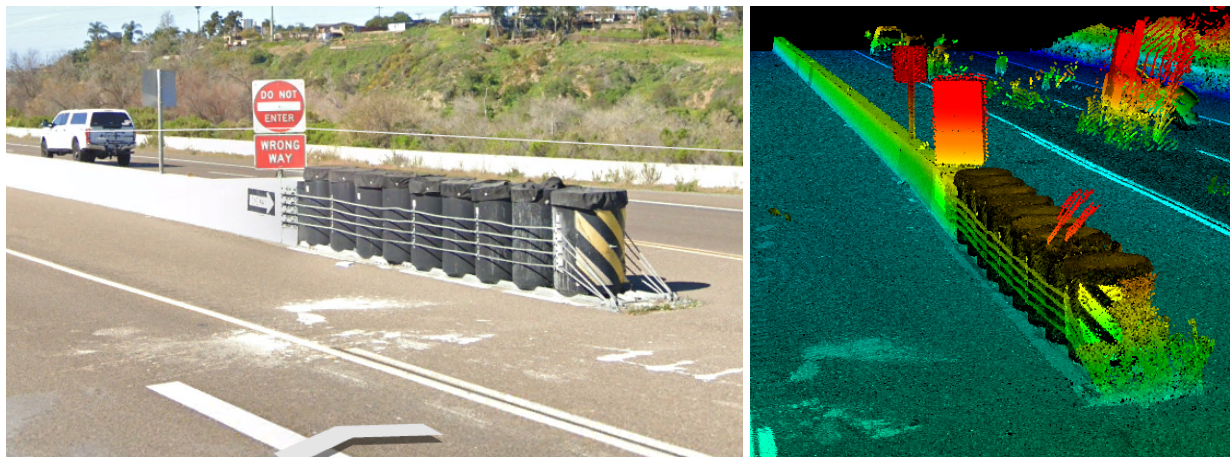
1. LiDAR: generates XYZ 3D points. The points not only have XYZ positional information but also intensity, color (RGB), and GNSS time tags etc., depending on the extent of processing.
2. Image or video: a 360-degree panoramic camera or multiple cameras.
3. Global Navigation Satellite System (GNSS): GNSS contains the position of the vehicle at the time of data acquisition. When combined, it provides the trajectory of the vehicle.
4. Inertial Measurement Unit (IMU): IMU provides the orientation or attitude of the vehicle.

Examining the point cloud data reveals the potential of extracting road-side features such as:

- Traffic signs
- Median divider
- Road markings
- Road condition
- Cross section

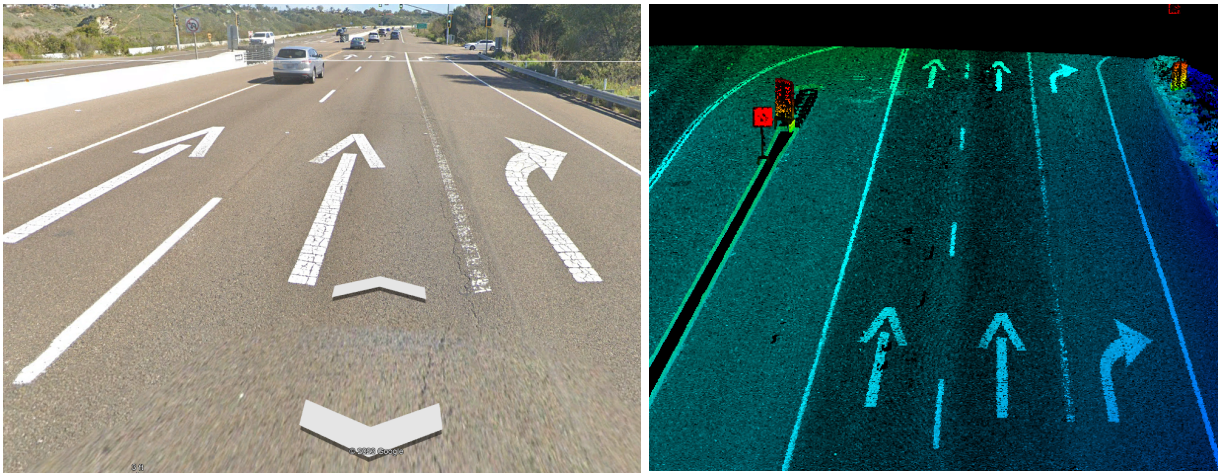
This information can be used for inventory mapping (Duffel and Rudrum, 2005).

Figure 2. Example of Traffic Signs and a Concrete Median Divider in Google Street Map (Left) and MTLs Point Cloud Data (Right)



The points in Figure 2 (right) are displayed by height (from blue to red) and intensity. Traffic signs, which are the objective of this study, and the concrete divider are clearly visible.

Figure 3. Example of Road Marks on Google Street Map (Left) and MTLs Point Cloud Data (Right)



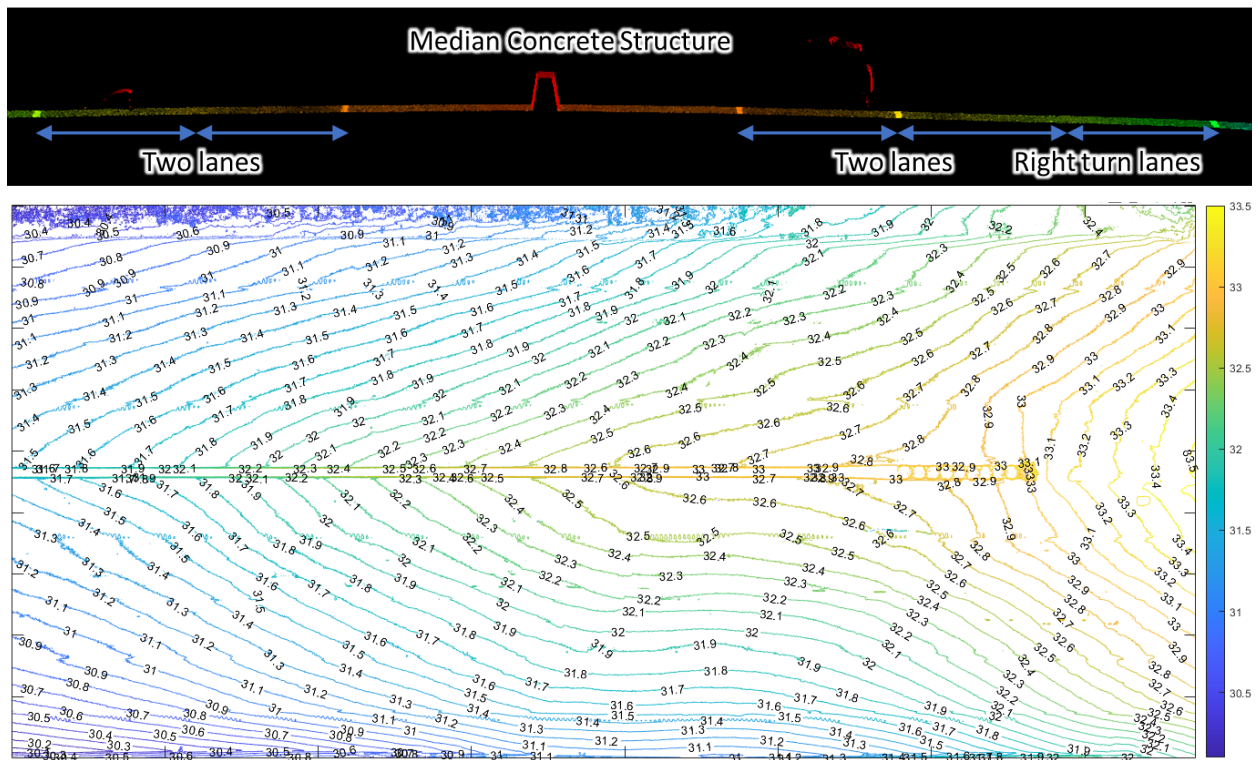
Standard solid lines, dashed skip lines, and arrow paints are clearly visible in the point cloud data (Figure 3). Point density of 400–500 points/ft², which is a common specification for MTLs used in transportation projects, enables a 2 cm resolution grid and can effectively extract the condition of the road marks.

Figure 4. Example of the Road Condition on Road Marks in the Google Street Map (Left) and MTLs Point Cloud Data



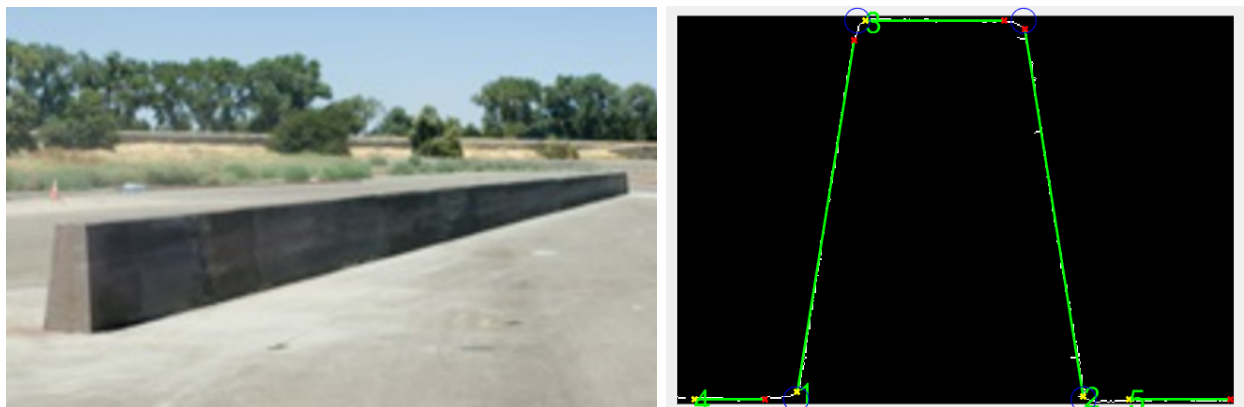
The point density is the function of scan speed, vehicle speed, and pulse repetition rate. When the speed is decreased to half of specified speed, one can achieve a higher point density than average point density. Figure 4 shows nearly 1,000 points/ft². This density of points provides the resolution of 1 cm or less, where road cracks can be clearly observed. The increased point density in the dataset is believed to be the results of the vehicle reducing its speed when passing a traffic signal.

Figure 5. Example of a Cross-Section in an MTLs Point Cloud (Upper) and a Detailed Surface Contour Representation



Median structure, slopes in both lanes, and road marks are clearly visible in the cross-section (Figure 5). The contour interval of 0.1 ft can reveal the detailed slope (Figure 6) and condition of the road's surface.

Figure 6. Example of Measuring the Dimensions of a Concrete Median Structural Barrier
Left: Photo of a Type 60 Median Barrier. Right: Extracted Lines and the Intersection of Those Lines for Dimension Calculations



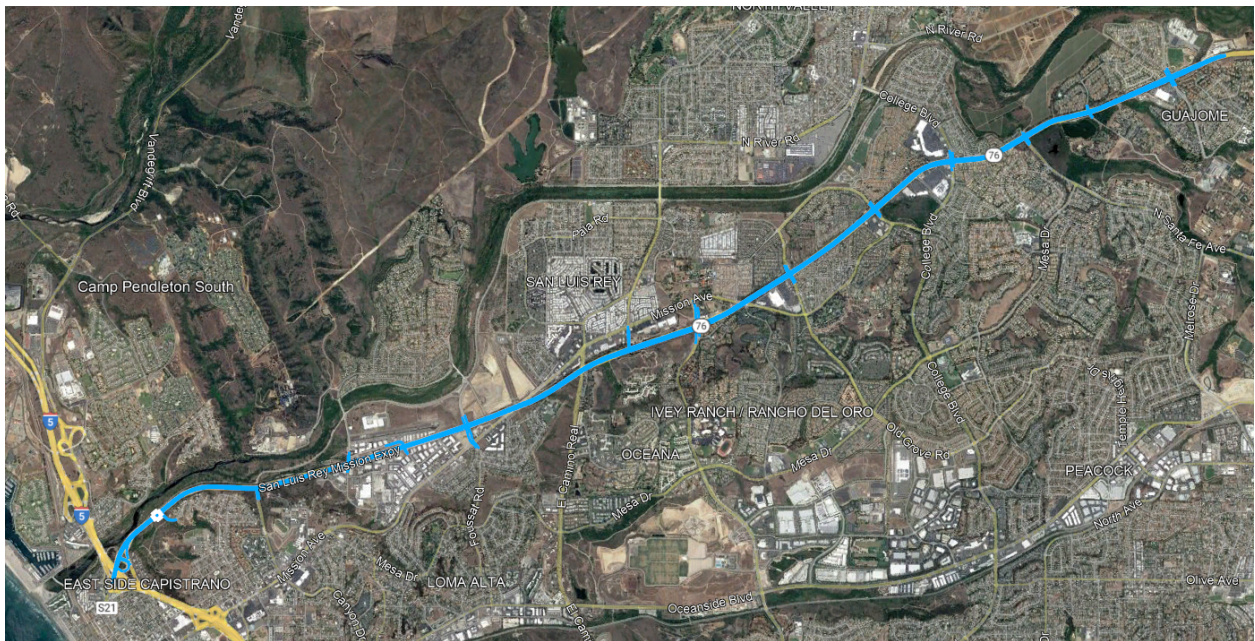
2.1 MTLs Dataset

The dataset was obtained on Highway 76, located between Los Angeles and San Diego, covering approximately 8.2 miles of road (Figure 7). The scans were executed multiple times, covering both the main highway (four times each direction) and arterial offshoots (two times each direction) (Figure 7). When combined, the total distance covered represents about 173 miles.

There is a total of 68 LAZ (compressed LAS) files: 8 files for main roads and 60 files for arterial roads. The total file size is 39.4 GB.

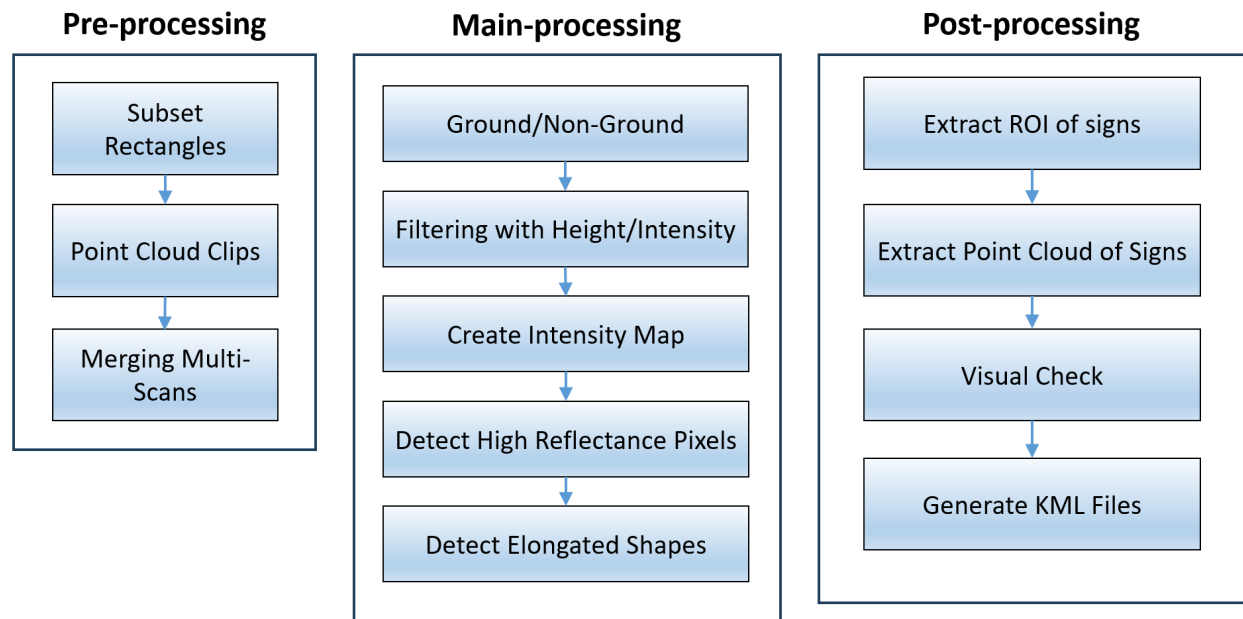
- 8 main roads: 4,404,701,236 points (4.4 billion)
- 60 secondary roads: 1,304,700,884 points (1.3 billion)
- Total number of points: 5,709,402,120 points (5.7 billion)

Figure 7. Trajectory Plot of MTLs Data on Highway 76
The Total Length is Approximately 8.2 Miles



2.2 Workflow

Figure 8. Workflow of Traffic Sign Extraction



The method to extract traffic signs consists of three major steps (see Figure 8): pre-processing, main-processing, and post-processing. In pre-processing, (1) merging multiple scans minimizes occluded area, (2) splitting the total length into 221 small rectangle boundaries eases computational load, and (3) filtering removes erroneous points or outliers. These steps in the pre-processing prepare the Mobile Terrestrial Laser Scanning data (MTLS) into manageable sizes, facilitating the detection of traffic sign areas.

The main steps involve: (1) separating ground and non-ground points to enforce the constraints that the traffic signs are located on non-ground points, (2) height filtering to remove points with a certain height above the specified traffic sign height, and (3) creating an intensity map. 3D points are grided in 2D to detect high intensity line segments that belong to traffic signs.

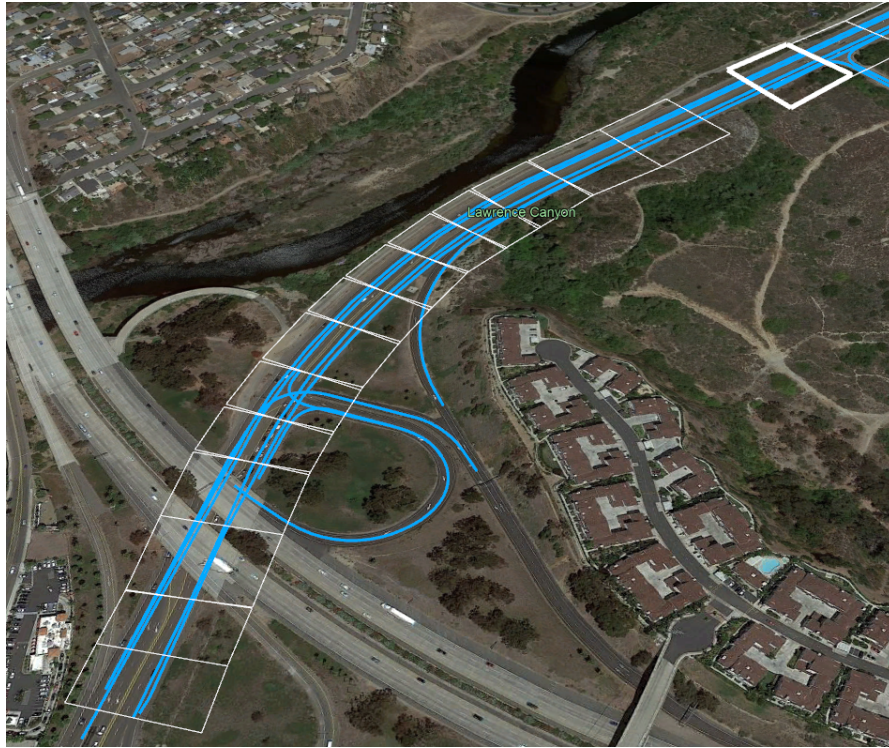
Finally, extracting points on traffic signs and calculating their central locations are performed. The locations of signs can be placed on the map and saved as a Keyhole Markup Language (KML) file which stores locations, image overlays, and modeling information such as shapes in programs such as Google Earth Pro. (see post-processing in Figure 8)

In the following three sections, these three steps are further explained with details.

2.2.1 Pre-Processing

The objective of pre-processing is to prepare the LiDAR dataset into a manageable size.

Figure 9. Illustration of Subset Rectangular Boundaries of LAS Files



To minimize computational load, a total of 221 rectangular boundaries were generated to cover the whole length of the data (see Figure 9).

The width (distance across the road) was set to 250 ft to cover not only the lanes but also the roadside features. Multi-scans are required to minimize shadow effects in the point cloud data and to increase the point density.

Figure 10. Example of a Shadow Effect in the LiDAR Scan. Left Lane Scan with Shadowed Right Lane (Left), Right Lane Scan With Shadowed Left Lane (Middle) and Combined Point Cloud (Right)

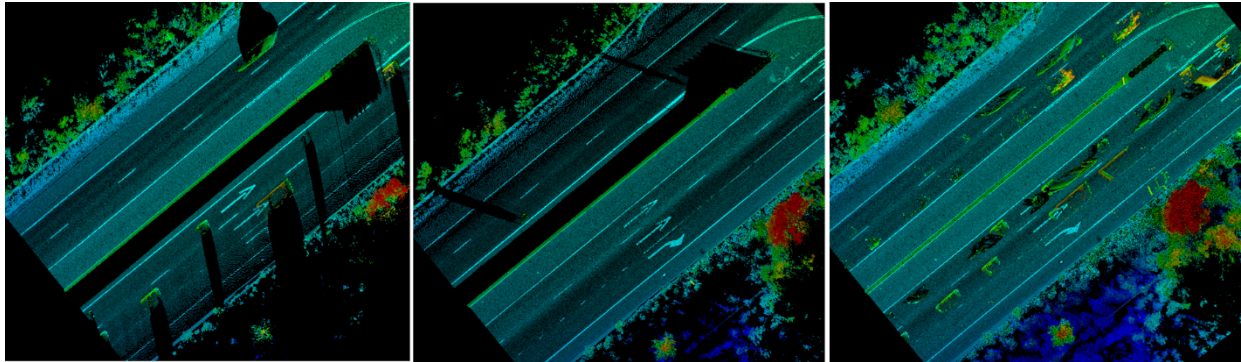
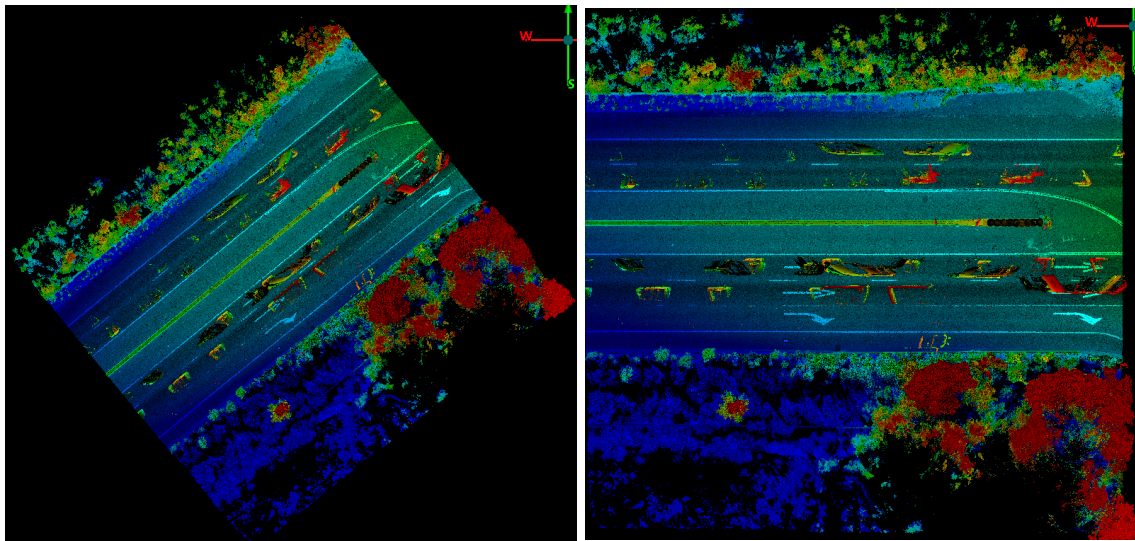


Figure 10 illustrates the shadow effect, where laser pulses are blocked by obstacles such as a median structure or other vehicles in the data-acquisition stage. When multi-scan data are merged, blocked areas are filled from other scans. Furthermore, merging increases the density of points, which increases the spatial resolution of the point cloud data

Figure 11. Screenshots of A Merged Subset (Left), and the Rotated Subset (Right)



The points within the rectangular boundary subsets were extracted from all 68 files and merged into single files. These subsets were also shifted and rotated so that they have local coordinates with smaller gaps outside of their boundaries (Figure 11).

These subset data contain 20–40 million points, which is manageable on a regular desktop computer.

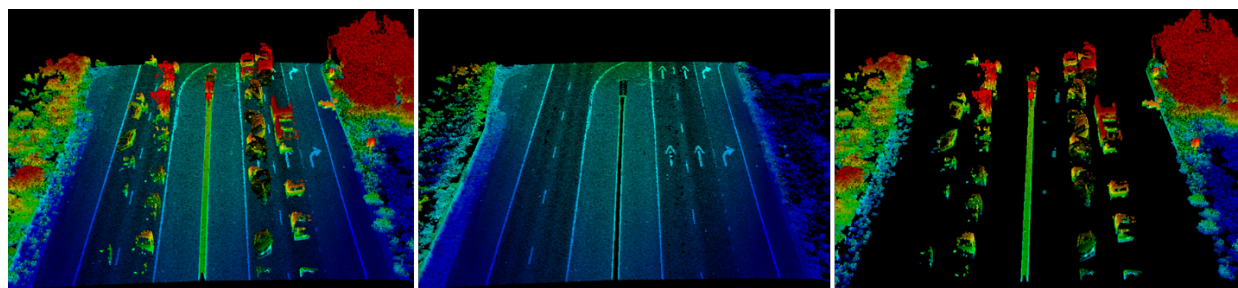
2.2.2 Main-Processing

Main-processing consists of ground/non-ground point separation, filtering for high intensity, generating an intensity map, thresholding to binarize the intensity map, and, finally, detecting elongated shapes.

Ground/Non-Ground Point Segmentation

Traffic signs are usually located in the middle or at the edge of the road, at a height ranging from 5 ft to 7 ft above the ground. However, in some instances, a “one way” arrow sign may be elevated only 1 foot from the ground. Regardless of the specific height, it is advantageous to have ground and non-ground points separated (refer to Figure 12). The MATLAB built-in function, “segmentGroundSMRF,” was used.

Figure 12. Original Mobile LiDAR Subset (Left), Ground Points (Middle), and Non-Ground Points (Right)



Intensity Map vs Digital Elevation Model

Traffic signs are manufactured to be retro-reflective to fulfill readability requirements during daytime and nighttime; this is known as “retro-reflectivity.” The Federal Highway Administration (FHA) provides a standard in the Manual on Uniform Traffic Control Devices (MUTCD) that requires agencies to maintain traffic signs to a minimum retro-reflectivity. This highly reflective surface on signs plays an important role in separating points on signs from other points.

Figure 13. Intensity Map (Left) and Elevation Map (Right). theLeft Panel Shows High Intensity, Colored Yellow, on Traffic Signs Whereas theElevation Map Does Not Show Strong Discernment

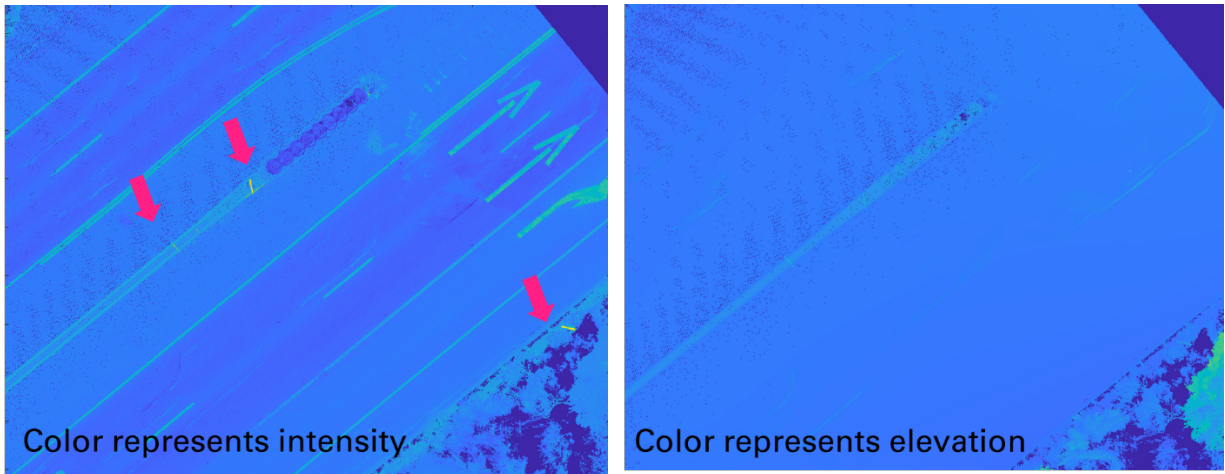


Figure 13 shows an intensity map and an elevation map. The point clouds were gridded with intensity and elevation with a resolution of 1.5 centimeters.

Figure 14. Histogram of Point Cloud Intensity

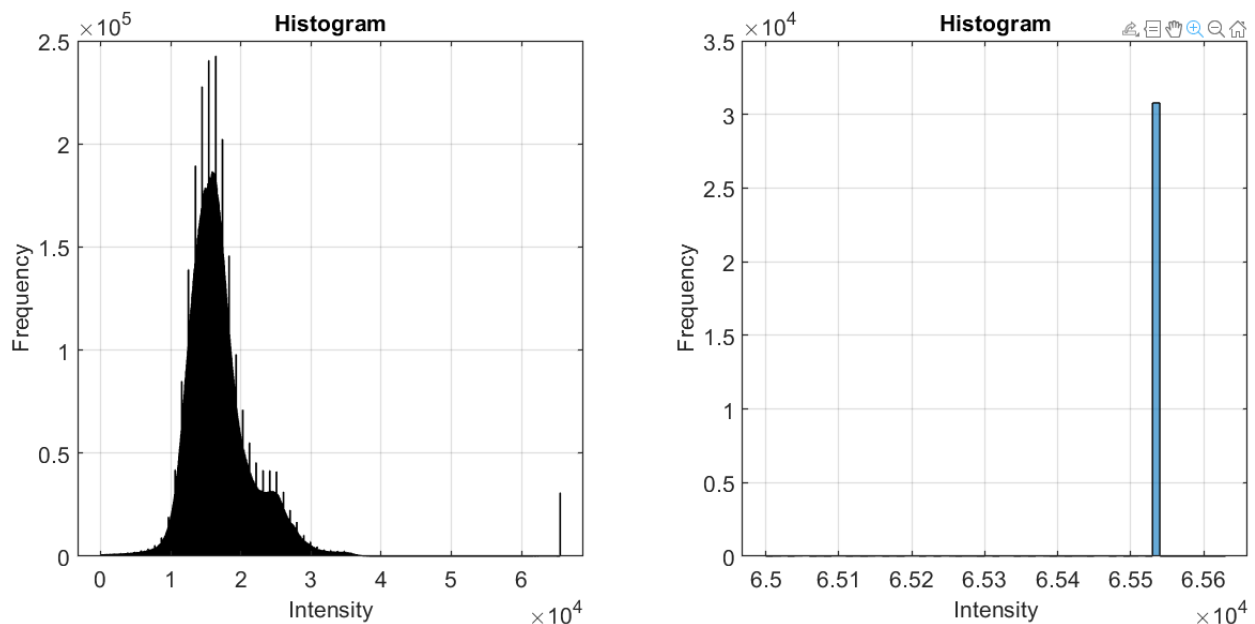


Figure 14 shows a small peak at the end of the intensity range. The points at this peak have the intensity value of 65,535 which is the maximum value of a 16-bit unsigned integer. This gives a good separation between points on traffic signs and others.

After analyzing point cloud density on roads and traffic signs (see Section III, Results and Analysis), the intensity maps were created with 0.05 ft (1.524 cm) resolution. Simple thresholding was enough to separate the regions of the signs, and minimum bounding rectangles were able to detect elongated rectangle shapes by checking their semi-major and semi-minor axis lengths.

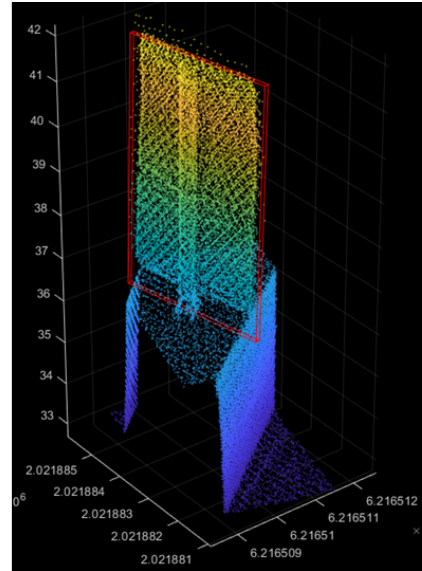
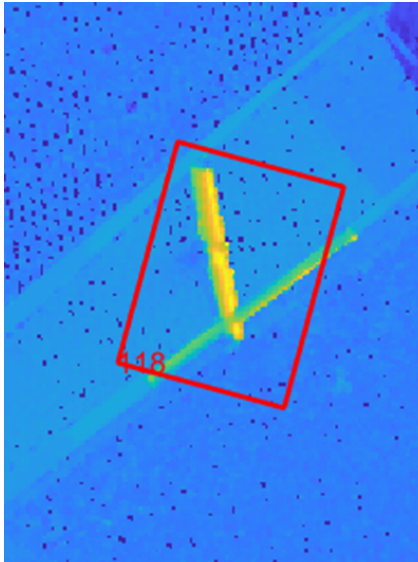
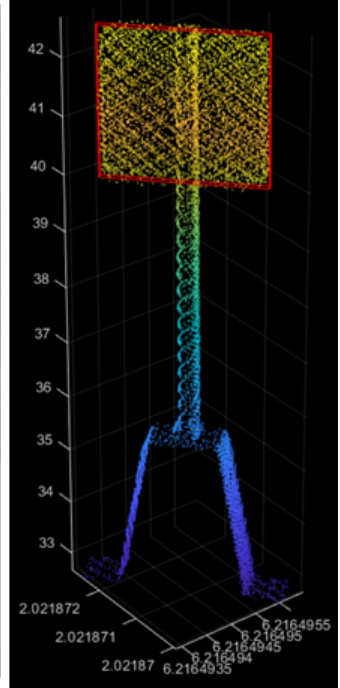
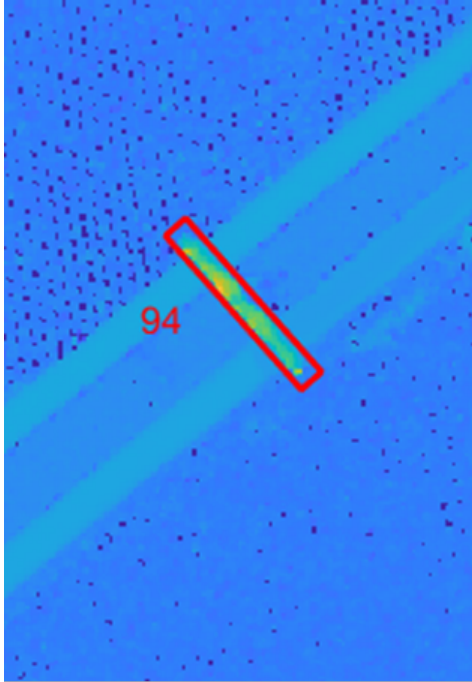
2.2.3 Post-Processing

Once high-intensity elongated-shaped pixels are extracted, a minimum length of 2.25 ft is applied to filter out some outliers. Then, all the points within that region of interest (ROI) are extracted. When the shape of a sign is a rectangle, one can go further to find the bottom and top of the sign by finding a height where the number of points abruptly jumps.

Best fitting planes using RANdom SAmple Consensus (RANSAC) provides points on the sign's plane. See the red 3D boxes in the point cloud display in the figures below.

Figure 15. High Intensity Rectangle Feature (Left), Actual Traffic Sign (Middle), and Extracted Point Cloud (Right) for Five Signs





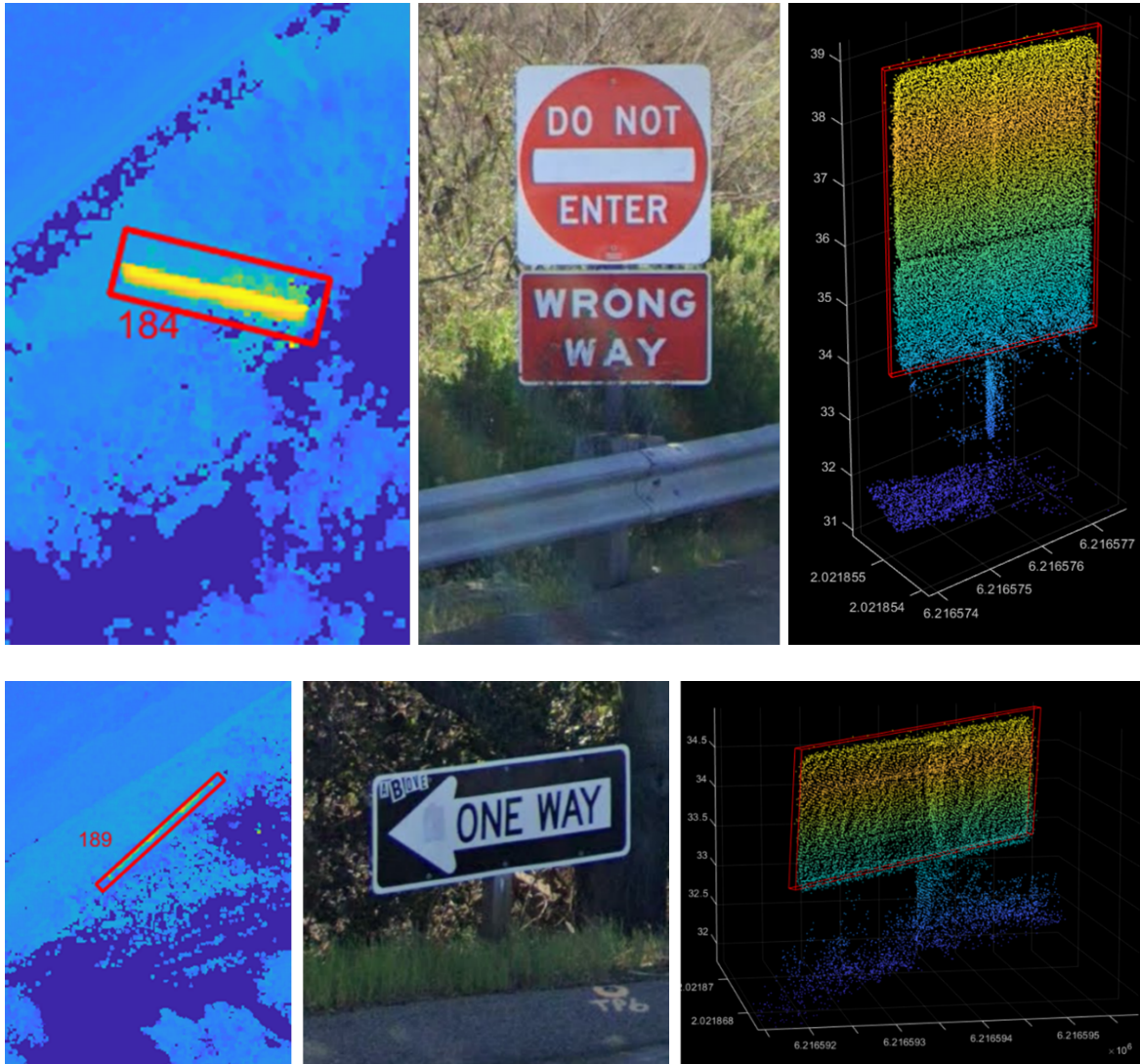
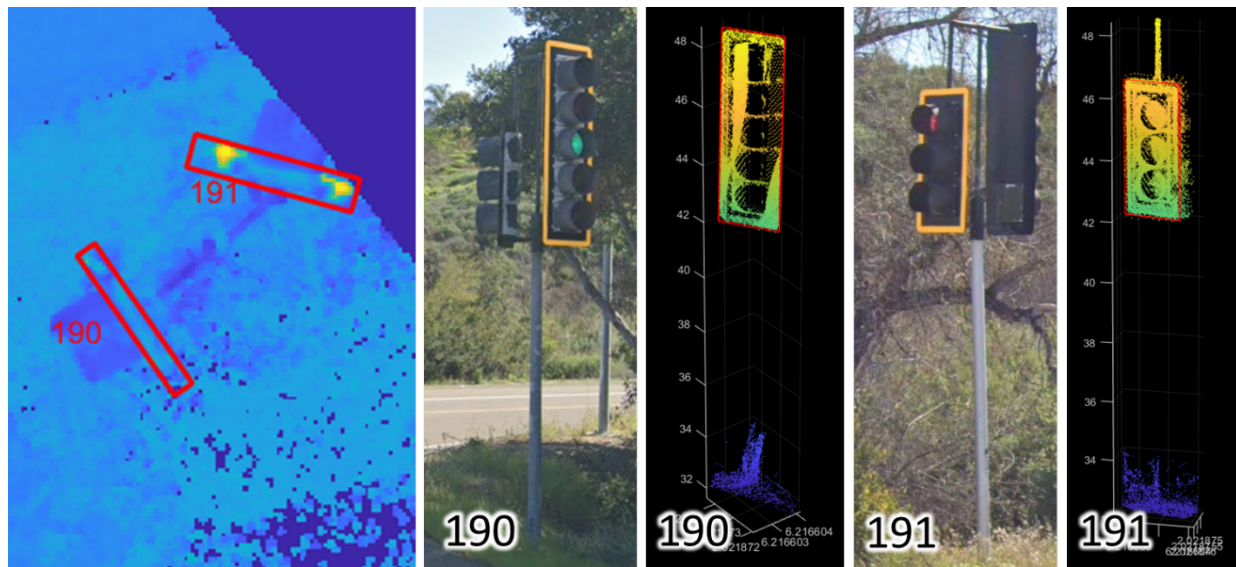


Figure 15 shows five traffic signs extracted from Subset 16. All the signs were extracted; however, it is observed that traffic signals were also extracted (Figure 16), since they pass the intensity filtering, shape filtering, and the height threshold condition. While they were not one of the objectives of this research, this study shows the possibility of detecting signals with pole structures from the Mobile LiDAR point data set. Figure 16 shows what traffic signals look like in intensity maps and the points extracted.

Figure 16. Extracted Traffic Signals



3. Results and Analysis

In this study, point density of aerial and mobile LiDAR data is analyzed to find the optimal resolution that can be produced from the points. The point density is a good indicator of the resolution of a grid map, which is simply a grid cell size. The equation (Hu, 2023) that defines the grid's resolution given the point density, for the Digital Elevation Model (DEM), is:

$$DEM\ resolution = \sqrt{\frac{1}{N}} \text{ ---- (1)}$$

where N is the point density, i.e., the number of points per unit area. For example, when there is 1 point per square meter, the optimal DEM resolution will be 1 meter (Garzon et al., 2021).

3.1 Aerial LiDAR vs. Mobile LiDAR

While aerial LiDAR data has relatively constant point distribution and point density over the area, Mobile Terrestrial Laser Scanning (MTLS) data has different distribution patterns. Simply, point density varies spatially, depending on the distance from the scanner, location, multi-scan pattern, and orientation of the targets.

First, aerial LiDAR data were downloaded from open topography (<https://opentopography.org/>), which is a public LiDAR data repository. It is 2014 USGS QL2 LiDAR, with 49,468 points.

Figure 17. Sample of Aerial LiDAR Data

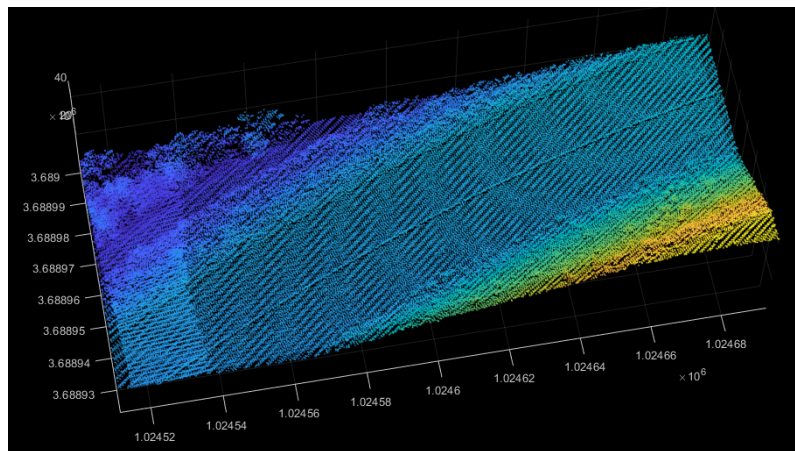


Figure 18. Point Density Map, Number of Points (Upper) and Resolution Map (Lower)

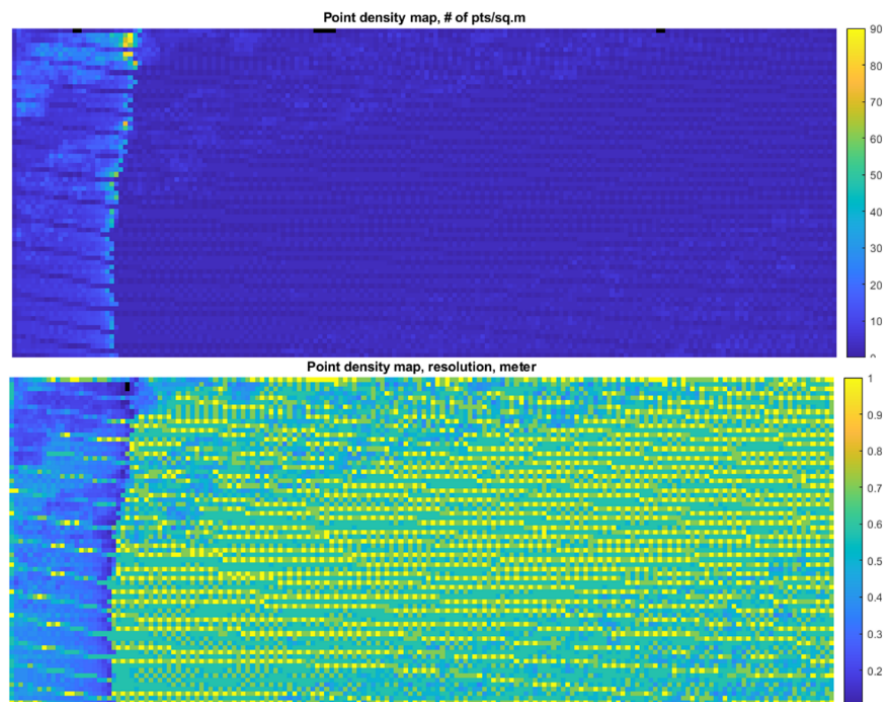
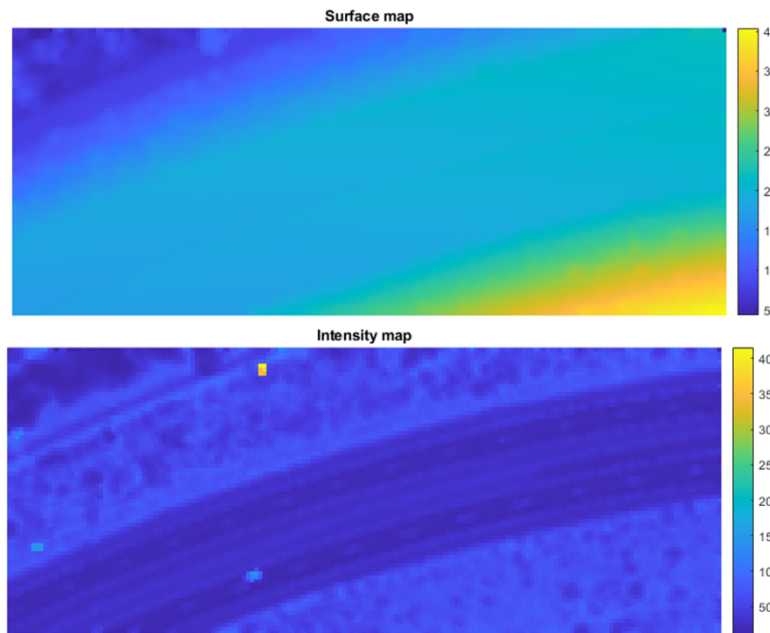


Figure 17 is the 3D plot of aerial LiDAR data. It shows that there is some amount of strip overlap on the left side of the figure.

Figure 18 shows a point density map where the pixels indicate the number of points in a cell. The cell size is 1 x 1 meter and most of the area has 1–4 points in a cell. Using equation 1, the grid resolution is calculated (Figure 18, lower). It shows that the 1-meter resolution (yellow color cell in Figure 18, lower) grid can be created. Figure 19 shows the Digital Elevation Model and Intensity map with 1 meter resolution. Smaller than 1 meter resolution will result in gaps and extrapolation effects.

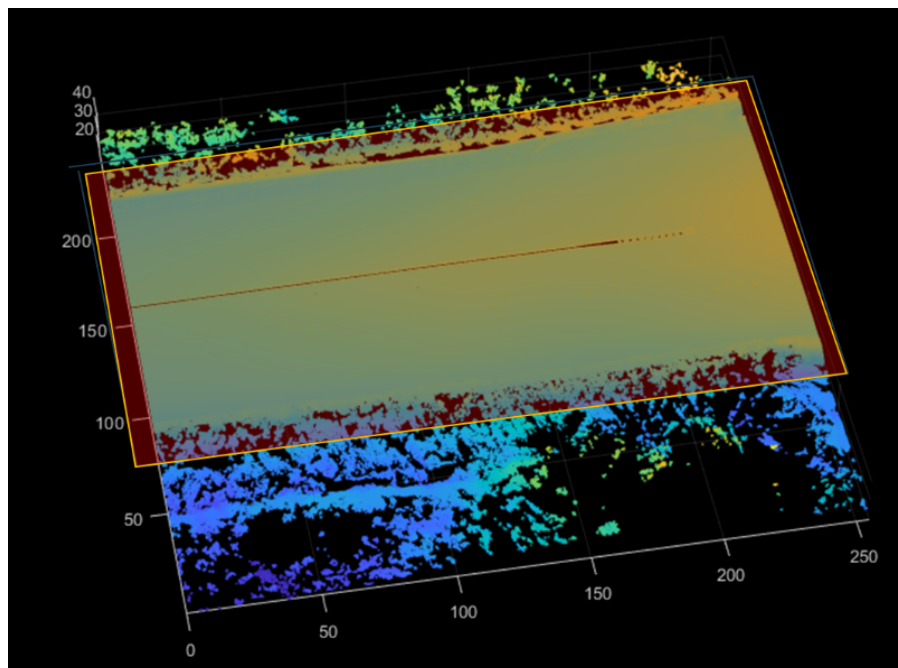
Figure 19. 1 Meter, Surface Map (Upper) and Intensity Map (Lower)



3.2 Point density on the road surface in Mobile LiDAR data

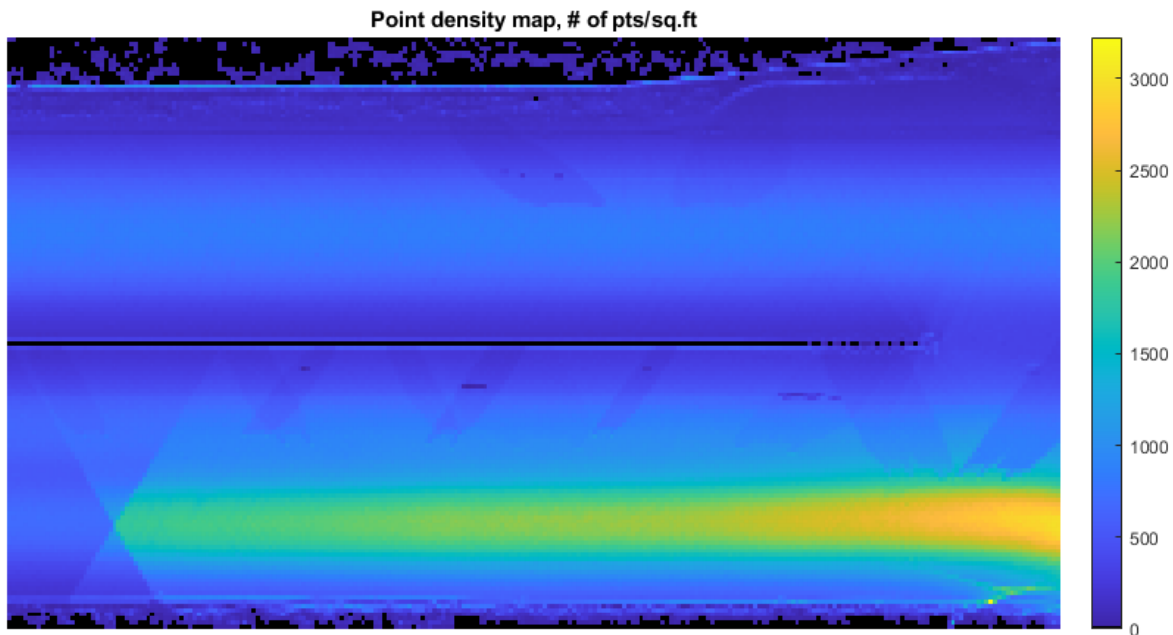
One subset from the Caltrans MTLs LiDAR data ($250 \text{ ft} \times 250 \text{ ft}$) was examined for density analysis. To analyze point density on the road surface, ground points were extracted (Figure 20).

Figure 20. Density Analysis, Mobile LiDAR Data



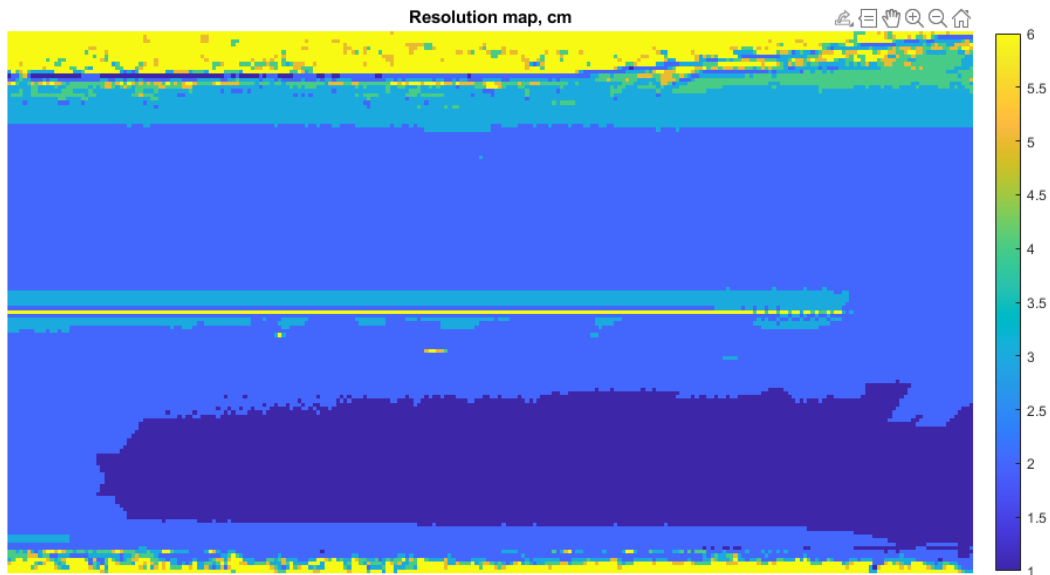
The number of points in the Mobile LiDAR data is 23,948,821 points and the area is 35,000 ft² (yellow rectangle). The average point density is therefore 684.25 points/ft² when divided by the area. The points are assigned to a 1 x 1 foot bin, and the number of points is counted. Since the data from multiple lanes are combined, the point density is not spatially consistent.

Figure 21. Point Density: Number of Points Per Sq. Ft.



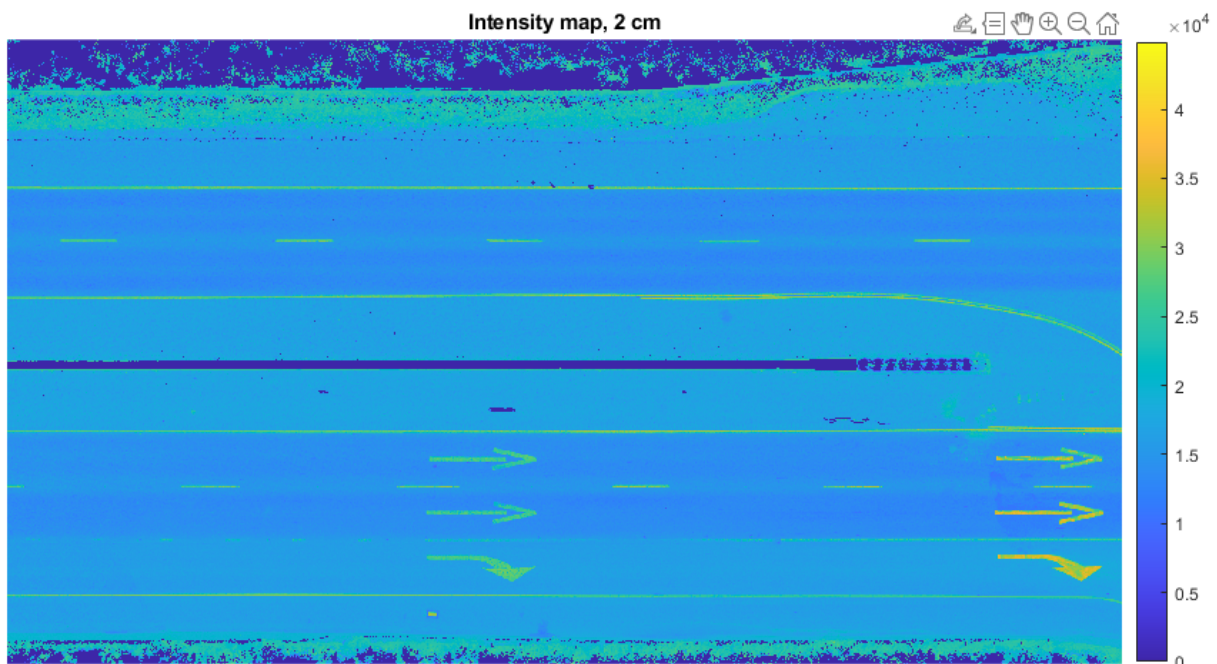
The yellow color in Figure 21 indicates that there are more than 2,000 points, but overall, the density is 500–1,000 points. It is believed that the scanner vehicle reduced its speed at the sight of a traffic signal. At normal speed, the Mobile LiDAR would receive 400–500 points per square feet.

Figure 22. Resolution Map



Based on the number-of-points map (Figure 21), one can produce a resolution map (Figure 22), which provides the optimal resolution of the surface from the Mobile LiDAR data. Note that locations with a bin of 2,000 or more points have a resolution of 0.5 cm, and for most of the road, 2 cm resolution surface can be generated.

Figure 23. Intensity Maps From MTLs Data. Resolution of 2 Cm (Upper), 1 Cm (Middle), and 0.5 Cm (Bottom)



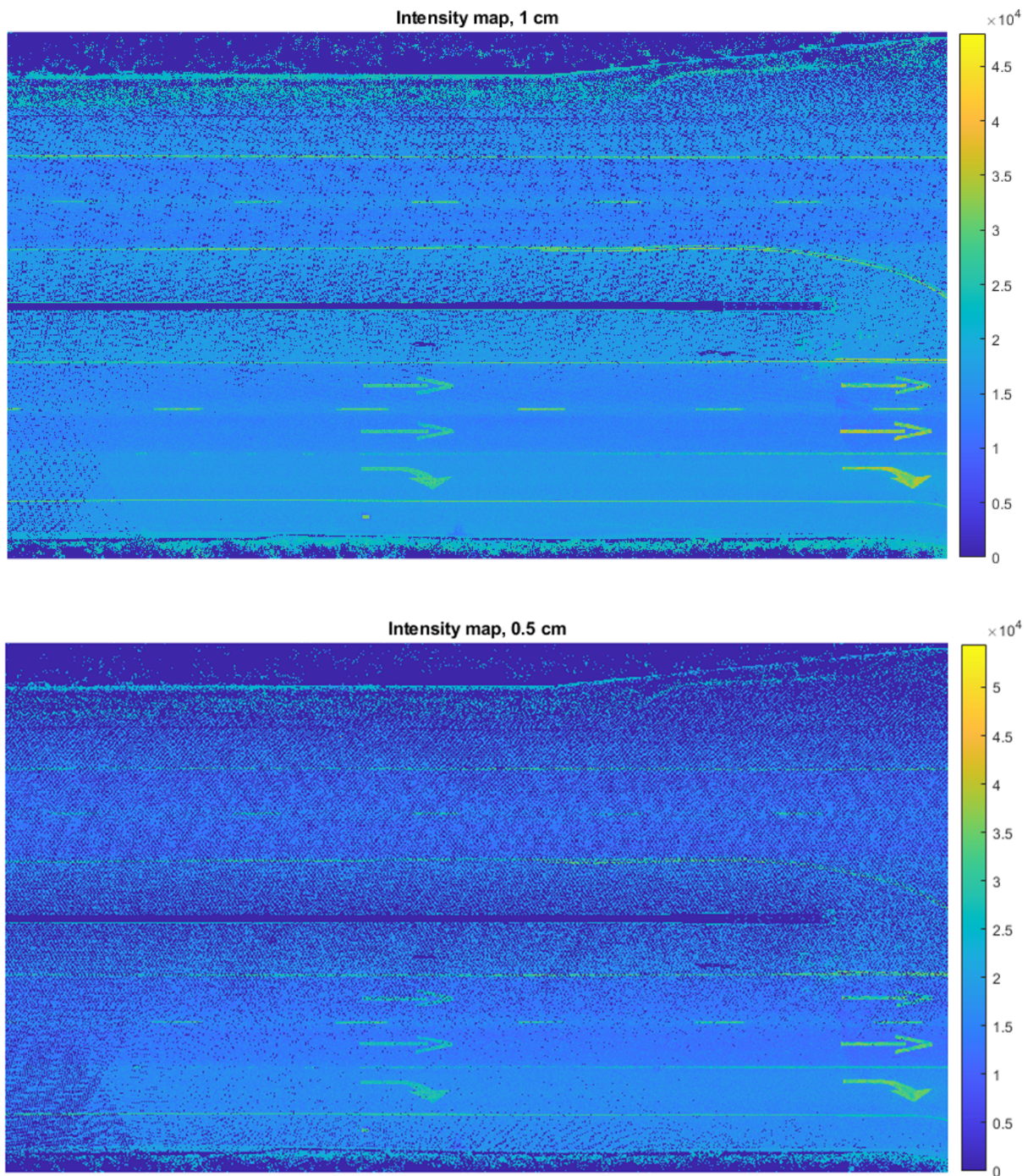


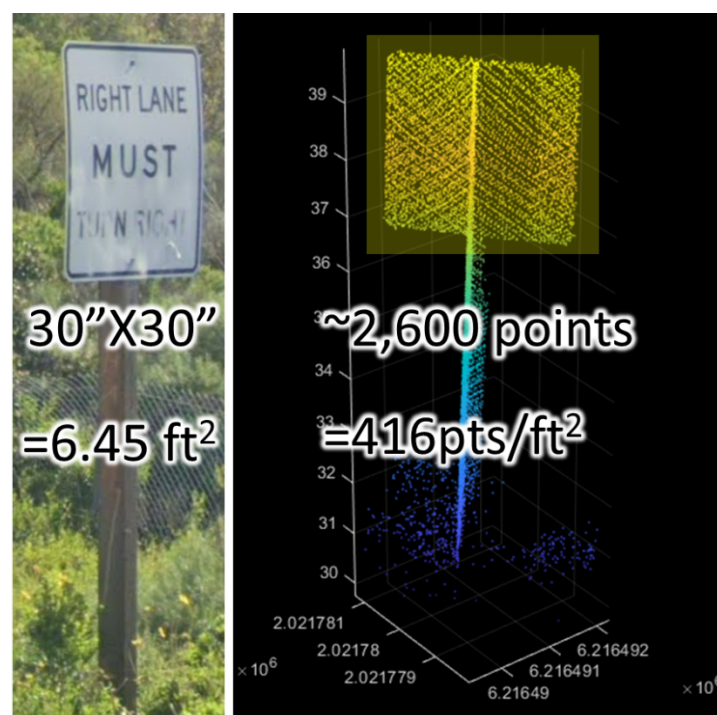
Figure 23 shows intensity maps with 2 cm, 1 cm, and 0.5 cm grid resolution. The bin where there are 2,000 points or more can generate a 0.5 cm resolution grid. Seven hundred points and more makes a 1 cm grid (right lane in figure 23), and most of the road can be covered by a 2 cm grid. Note that, when needed, a 0.5 cm resolution area will show the road condition better, such as cracks and detailed surfaces.

3.3 Point density on traffic signs

The mobile scanner scans along the road multiple times to avoid shadow effects where laser signals are blocked by obstructions such as median structures or other vehicles. This multiple-scan property inevitably results in inconsistent point density. This applies to traffic sign cases.

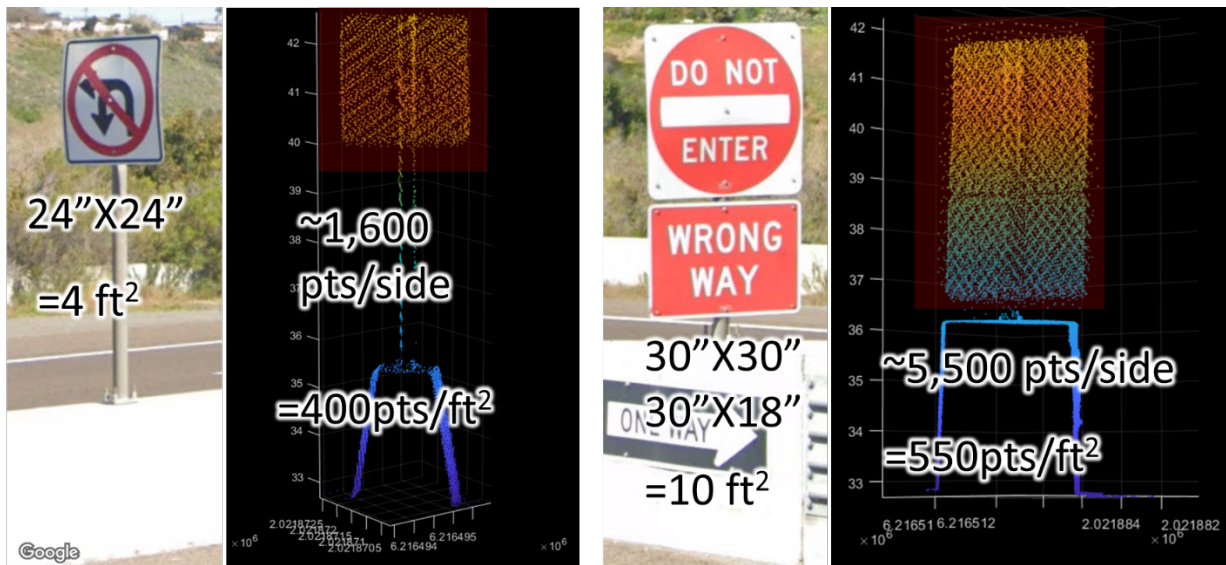
Depending on incident angles, distance from the scanner to the targets, target sizes, and the speed of the scanner vehicle, each traffic sign has a different number of points. Three signs were extracted and analyzed for their point densities.

Figure 24. Point Density of Sign I



Sign I has dimensions of 30"×30" (762mm×762mm), a square sign (Figure 24). There are 2,600 points on the target whose area is 6.45 ft². The density is therefore 416 points/ft² (4476 points/m²).

Figure 25. Point Density of Signs II and III



Sign II is 24"×24" in size and Sign III (consisting of two signs) has 30"×30" and 30"×18" dimensions (Figure 25). When divided by the number of points, the point densities are 416 points/ft² and 550 points/ft², respectively.

3.4 Traffic sign extraction

The traffic sign extraction procedure described in Figure 8 in Section 2.2 is applied to the merged subsets. First, Subset 16, where various signs were observed, was tested.

Figure 26. Ground Truth Signs In Subset 16

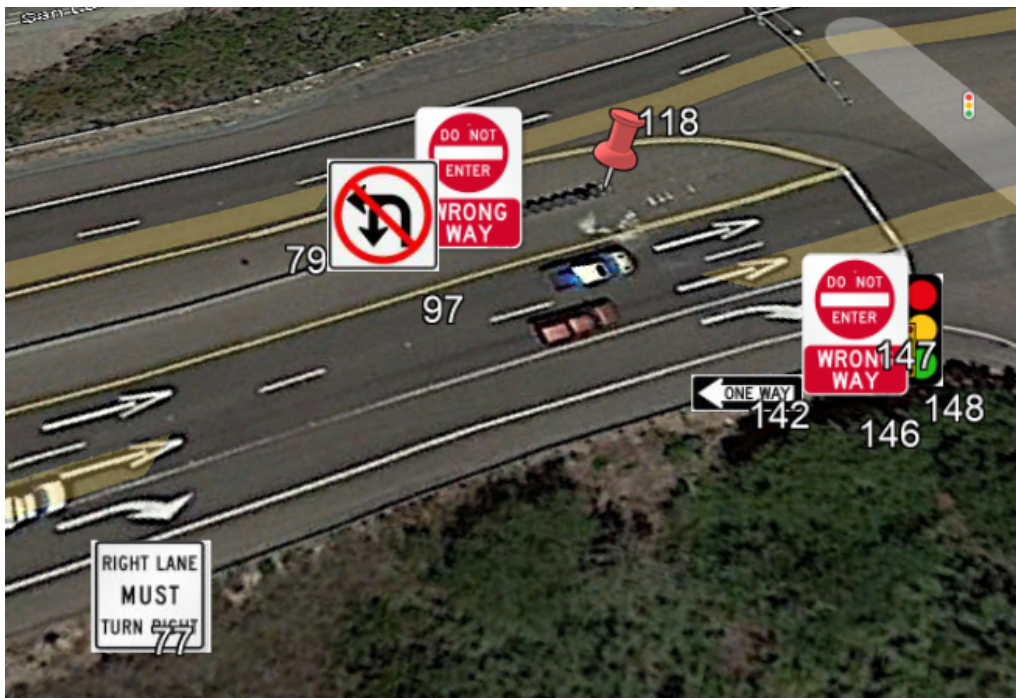


Figure 27. Extracted Signs, Subset 16

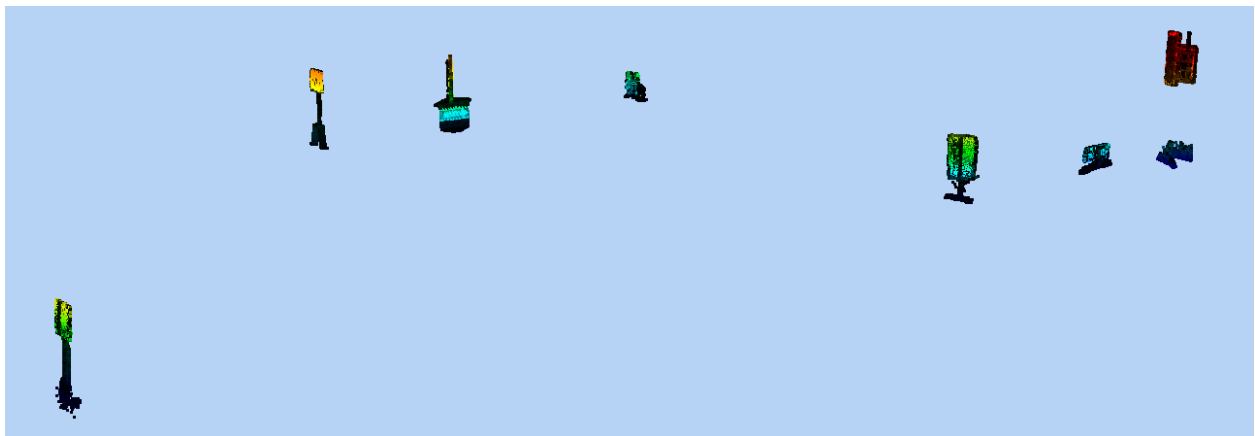
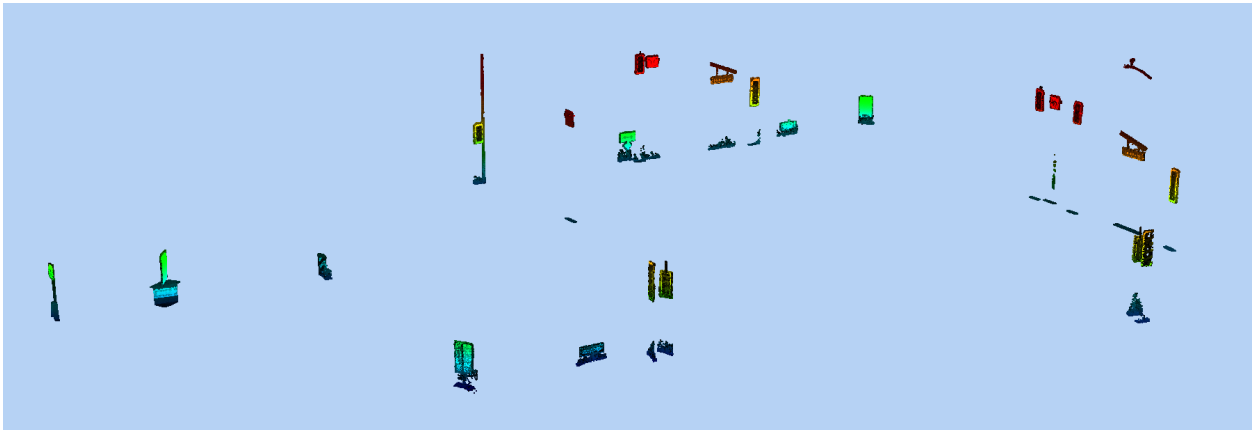


Figure 26 shows manually identified signs, and Figure 27 shows extracted traffic signs using intensity-based extraction.

Figure 29. Front View of Extracted Traffic Signs and Traffic Signals in Subsets 10–20



Figure 30. Side View of Extracted Signs and Traffic Signal in Subset 10–20



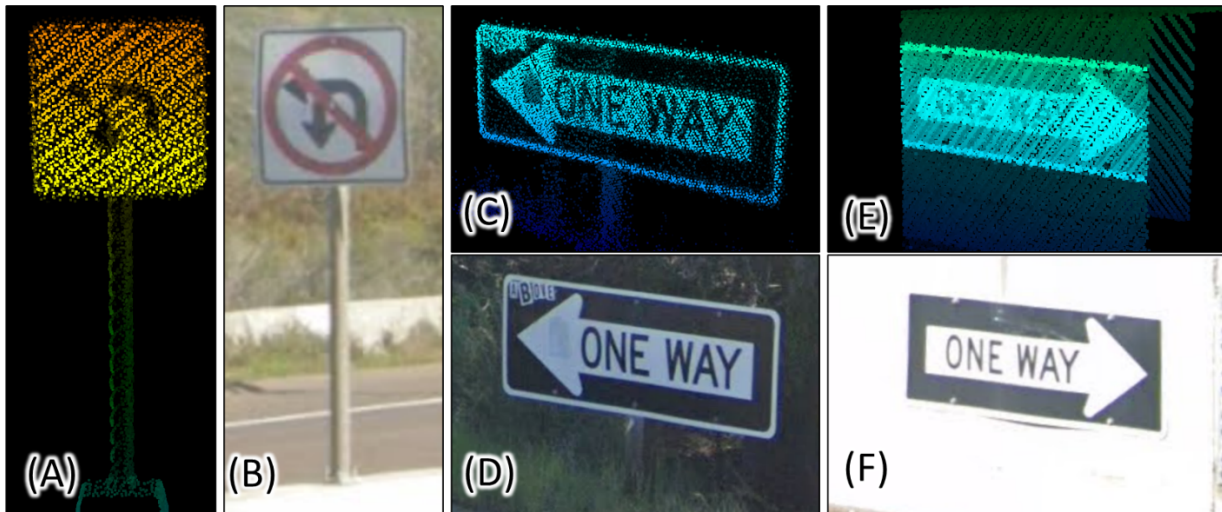
Figures 29 and 30 show the results of processing 10 subsets, subset 11 to subset 20. A total of 57 signs are extracted.

Table 1. Traffic Sign Extraction Results, Subsets 11–20

	Existing Signs	Extracted Features	Extracted Signs	Vehicle	Traffic Signals	(Water Tank)	Sign Success
Subset 11	1	1	1				100
Subset 12	2	3	2	1			100
Subset 13	2	2	2				100
Subset 14	4	4	4				100
Subset 15	0	0	0				100
Subset 16	5	8	5		2	1	100
Subset 17	8	18	8	1	8	1	100
Subset 18	1	1	1				100
Subset 19	3	3	3				100
Subset 20	2	2	2				100
Total	28	42	28				

Table 1 shows existing signs and extracted signs for the subset 11–20. There are 28 traffic signs in total, and all the signs were extracted. The column “Extracted features” indicates the number of features extracted, which include: (1) points on a vehicle, (2) traffic signals, and (3) miscellaneous, such as a water tank on the road median.

Figure 31. Colors on Traffic Signs



When black and white paint occurs on signs, it is observed that black paint reflects less intensity back, whereas high intensity is reflected back from white paint. In this case, the shape, such as the shape of arrows or often letters, can be identified. Note that the intensity of red paint is similar to white paint. Figure 31 (A) and (B) show a “no-left turn/no U-turn” sign. It is seen that the black-colored arrow has low intensity, providing a visually identifiable shape. (C)/(D) and (E)/(F) are “one-way” signs that have only black and white colors with large letters on them. The density of 400–500 points/ft² on the sign is enough to read it.

4. Summary and Conclusion

This research explores the detection of traffic signs using Mobile LiDAR point cloud data. The intensity-based sign extraction method effectively identifies traffic signs, traffic signals, and other retro-reflective objects, offering valuable insights for transportation asset management. The workflow initiates with the management of the LAS dataset, involving tasks such as merging/splitting, gridding, and detecting high-intensity features. Subsequently, the identified signs are placed in Google Earth Pro, facilitating their seamless display in Geographic Information Systems (GIS).

This study delves into the analysis of point density, establishing a connection with potential grid resolutions that allow for additional extraction or analysis, such as road condition assessments or crack detection.

In addition, the research investigates deep learning point classification and Hough transformation plane detection (see the Appendices). The outcomes and limitations of these approaches are summarized.

While detecting and localizing the traffic signs in this study show promising results, it lacks the ability to identify signs. Simply, point cloud solely doesn't provide a way to read the signs. This limitation comes from the characteristics of point cloud and necessitates the use of image (or video) data for future work.

Appendix A

Appendix A summarizes 1) line and plane detection from point cloud data using Hough Transformation and 2) the Visual C++ program that reads, writes, thresholds by elevation and intensity values, and detects planes.

Hough Transform for 2D Line Detection:

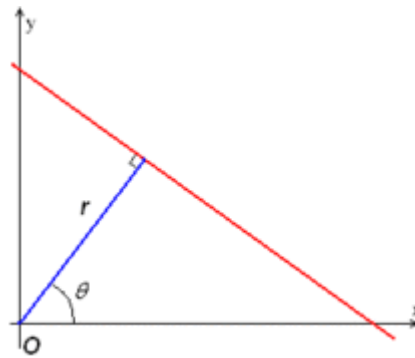
Using the parametric line equation:

$$r = (x - xc)\cos\theta + (y - yc)\sin\theta$$

$$r - r_o = x \cos \theta + y \sin \theta$$

$$r_o = xc \cos\theta + yc \sin\theta \text{ --- (A1)}$$

Figure 32. 2D Hough Transformation Space



The 2D Hough Space is defined as (θ, r) space.

3D Hough Transform for Plane Detection:

Planes are commonly represented by the following parametric equations:

$$AX + BY + CZ + D = 0 \text{ --- (A2)}$$

Or:

$$Z = m_x X + m_y Y + \rho \text{ --- (A3)}$$

$$\rho = X \cos \theta \sin \varphi + Y \sin \theta \sin \varphi + Z \cos \varphi \text{ --- (A4)}$$

Where:

ρ : signed distance to the origin of the coordinate system

m_x : slope in x-axis direction

m_y : slope in y-axis direction

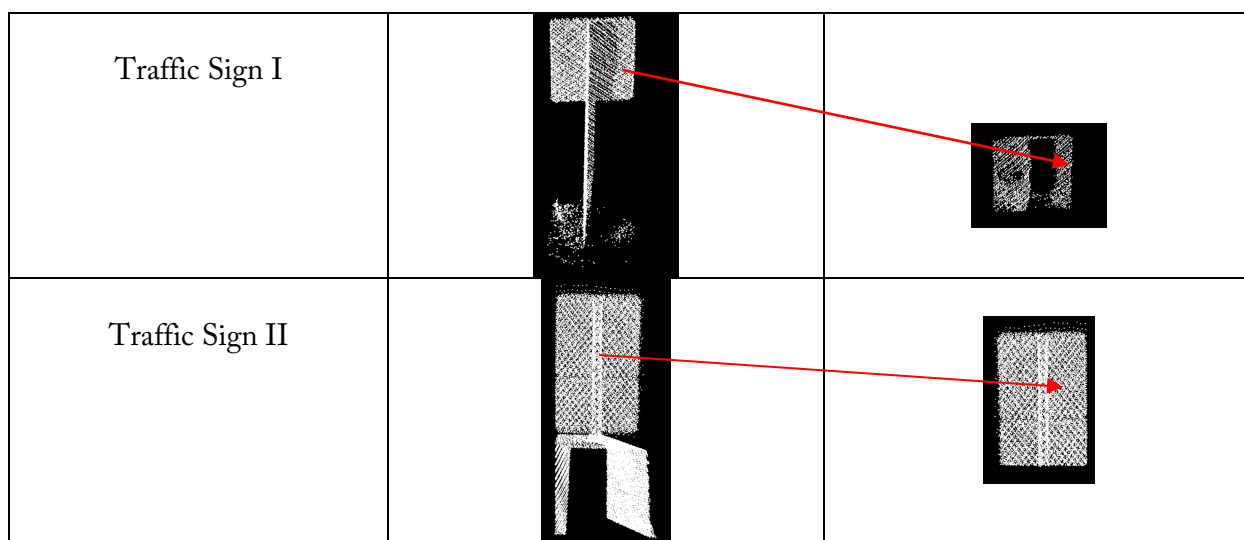
X, Y, Z: Cartesian point coordinates

θ : The angle of the normal vector on the xy-plane

φ : The angle between the xy-plane and the normal vector in the z direction

The 3D Hough Space is defined as (θ, φ, ρ) space.

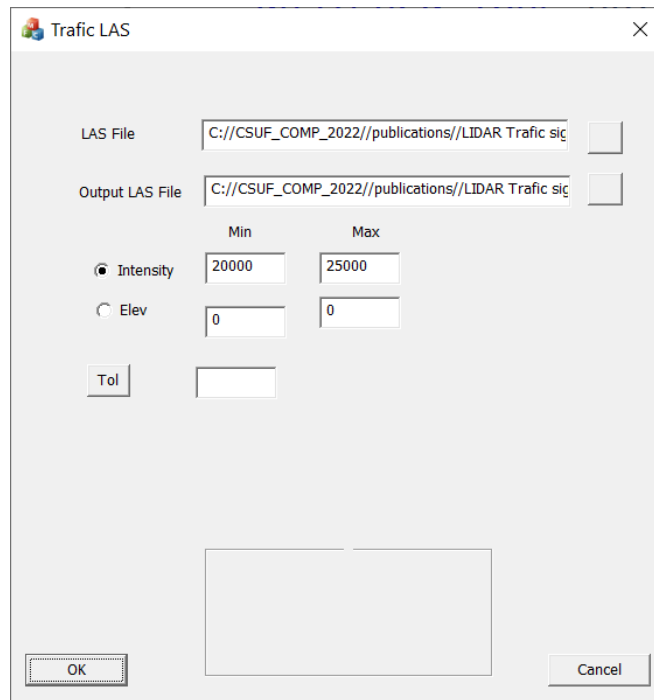
Figure 33. Example of Plane Detection Using Hough Transformation



The algorithm was effective when the 3D point cloud was defined with bounded intensity and elevation. Otherwise, multiple planes interfere with each other.

Future work such as least squares adjustment for the 3D point cloud fit for the 3D plane will improve the results and minimize the noise of the results. Also, line intersection between planes will help define the traffic sign region.

Figure 34. Traffic LAS Visual C++ Program



A Visual C++ program was developed to evaluate the potential of using LIDAR intensity to detect traffic signs (Figure 34). The main features of the program are as follows:

- Read LAS files;
- Write LAS files;
- Set up LiDAR intensity range;
- Set up 3D point cloud elevation range; and
- Detect 3D point clouds that form planes.

Future work:

- 3D point cloud least squares adjustment for the 3D plane;
- 3D plane intersection to define the traffic sign boundary;
- Integrate the RGB camera data with the LIDAR intensity; and
- Use RGB data with LiDAR intensity to enhance the traffic sign detection algorithm and use it for sign classification.

Appendix B

In this study, Deep Learning using PointNet++ in MATLAB to classify road points was tested.

PointNet++

PointNet represents a deep-learning model designed for processing point cloud data, exhibiting proficiency in three distinct classification tasks: classification, part segmentation, and semantic segmentation. In the context of classification, PointNet excels at categorizing objects into specific groups, distinguishing, for instance, between individuals and vehicles. Part segmentation involves dissecting a singular object into its various components, exemplified by the ability to identify windows, tires, and bodies when classifying a car. Semantic segmentation, akin to part segmentation, deals with point clouds lacking clear boundaries; however, it is specifically applied to categorize elements within the background environment. This includes identifying features such as traffic lights, asphalt roads, sidewalks, and vegetation.

Point Cloud Data Pre-Processing

CloudCompare, open-source point cloud processing software, was used to test PointNet classification. Multi-lane data were combined into one file. This helps minimize gaps in the data.

Most of the point cloud classification research uses Airborne point cloud data. Airborne point cloud data has the advantage that it can cover an area quickly and with spatial consistency, but it sacrifices details. On the other hand, Mobile LiDAR data can provide better details but the point distribution and density vary. Viewing angle from a vehicle also has adverse effects on manually making a training dataset for Deep Learning. Large file size also limits using PointNet as it is. Therefore, outliers are manually filtered and points are averaged so that similar point density is maintained over the test area. Below is the summary method of pre-processing the point cloud data.

1. Combine point cloud files using CloudCompare.
2. Average point cloud density using 'Remove Duplicate Point Cloud' with a minimum distance of 0.05 ft.
3. Delete insufficient point cloud data in the file.

An example is shown in Figure 35. The left image is an example of what needs to be deleted. The right image is an example of what remains after deleting all the unnecessary data.

Figure 35. Example of Manual Filtering Pre-Process. Left Panel Indicates Area of Filtering and Right Panel Shows the Results After Filtering

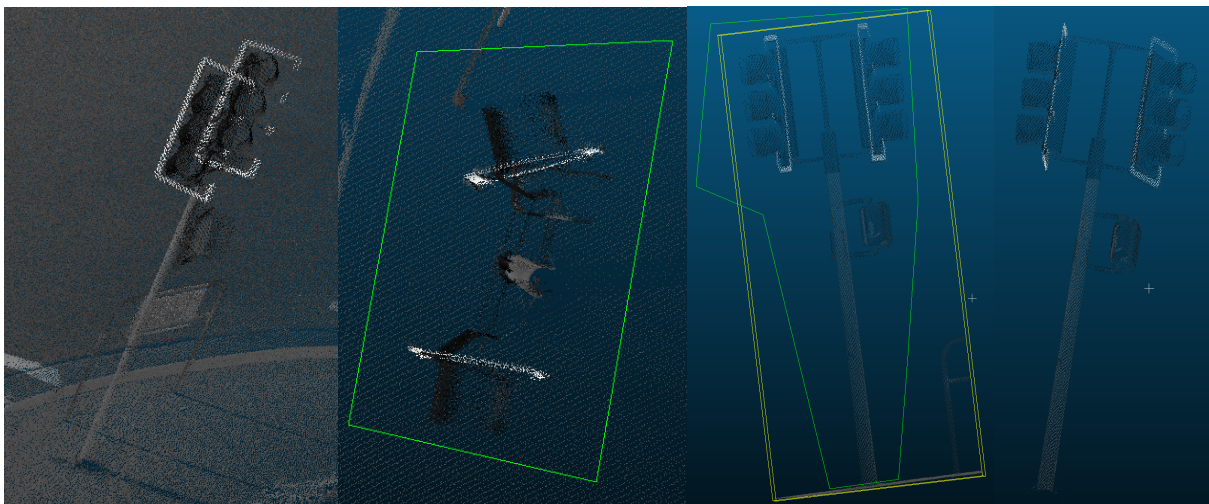


Classify data

Define categories.

- Use the segment function in CloudCompare to isolate point clouds based on the defined categories. It is hard to isolate a clean object. It usually requires users to repeat this process many times from different points of view until a clear object from the environment has been achieved.
- Mark all the point clouds with a value under the SF label Classification. This value represents the category (or class) of the point cloud.

Figure 36. Example of Manual Definition of Categories. Traffic Light and Pole are Delineated and Labeled



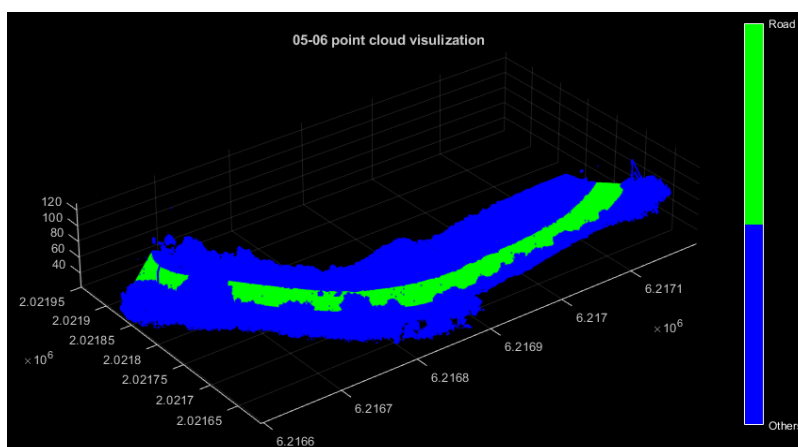
Coding Configuration

PointNet was originally implemented in Python. Some of the components need to be run on the Linux system. MATLAB has a copy version of PointNet++ that can run on the Windows operating system. For more detail please reference the example *Aerial LiDAR Semantic Segmentation Using PointNet++ Deep Learning* <https://www.mathworks.com/help/lidar/ug/aerial-lidar-segmentation-using-pointnet-network.html> .

The details and the key terms will be explained. The code in *Semantic Segmentation Using PointNet++ Deep Learning* can be broken down into seven parts. Load Dayton Annotated LiDAR Earth Scan (DALES) Data, Pre-Process Data, Create Datastore Object for Training, Define PointNet++ Model, Specify Training Options, Train Model, Segment Aerial Point Cloud, and Evaluate Network.

The first code is Load DALES Data. This is the code that will load the point cloud file and display the classification. If the file or the classification cannot be displayed, it indicates the file is not in a format that the code can read. This needs to be fixed before proceeding. There are variables that are important in Load DALES Data. They are dataFolder, trainDataFolder, testDataFolder, and classNames. The variable dataFolder is the directory that includes the other two folders trainDataFolder and testDataFolder. trainDataFolder is the directory that includes all the labeled data sets that can be used for the training. testDataFolder is the folder that includes other sets of labeled data that can be used to verify the model. className is the label for the classifications. If everything is correct, the result should display the classified point cloud data. An example is below (Figure 37). If the label of the color is not correct, try to inverse the order of the classNames.

Figure 37. Labeled Point Cloud Data Sets in MATLAB



The second code, Pre-Process Data, in the Matlab example has a variable named blocksize. The code will process one file at a time but point cloud file is usually large and will take a lot of memory. The solution to this is to separate one large file into many small blocks. The variable 'blocksize' is

used to define the block size. For a regular ground surface point cloud, the Z direct size is usually infinity. Users only need to define the X and Y dimensions. For example, to define an area of 51 times 51 will be blocksize = [51 51 Inf].

For the code, Create Datastore Object for Training, Define PointNet++ Model, and Specify Training Options, nothing needs to be changed.

At code, Train Model, the boolean variable 'doTraining' decides the code operation. If variable doTraining is false, it will load the model and perform segmentation on the test data set and return the statistic of its accuracy. If variable doTraining is true, it will use training datasets to train a new model.

Analysis

Our classification includes seven categories. They are Others, Vehicle, Asphalt_Road, Traffic_Sign, Sign_on_TL, Traffic_Light, and Lamp. We feed six files to train the model. Figures 38 to 40 show the results we obtained from the training, whereby IoU (Intersection over Union) is a performance metric commonly used in object detection.

Figure 38. Trained Result Based on Our Labeled Data 1

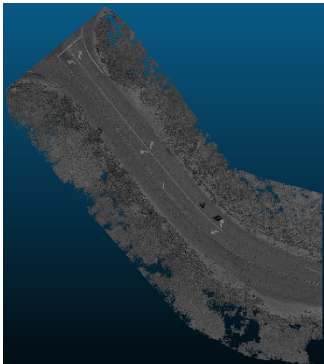
	Accuracy	IoU	
Others	0.96247	0.93349	
Vehical	0	0	
Asphalt_Road	0.90179	0.79428	
Traffic_Sign	0	0	
Sign_on_TL	NaN	NaN	
Traffic_Light	0	0	
Lamp	0	0	

Figure 39. Trained Result Based on Our Labeled Data 2

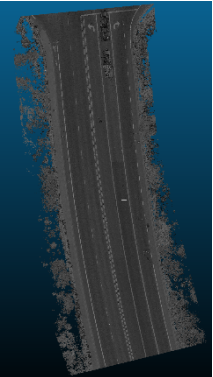
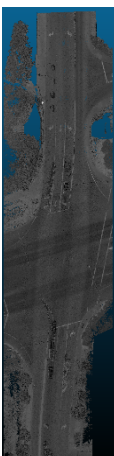
	Accuracy	IoU	
Others	0.61621	0.60279	
Vehical	0.746	0.73245	
Asphalt_Road	0.99033	0.8053	
Traffic_Sign	0	0	
Sign_on_TL	NaN	NaN	
Traffic_Light	0.084631	0.070895	
Lamp	0.30759	0.29652	

Figure 40. Trained Result Based on Our Labeled Data 3

	Accuracy	IoU	
Others	0.62532	0.54527	
Vehical	0.18777	0.049497	
Asphalt_Road	0.89763	0.78892	
Traffic_Sign	0	0	
Sign_on_TL	0	0	
Traffic_Light	0.82841	0.27877	
Lamp	0.36447	0.3425	

Upon analyzing the statistical outcomes, it is evident that PointNet++ is effective. Notably, the segmentation of asphalt roads achieves the highest accuracy, surpassing 80% according to verification statistics. However, the accuracy of other categories appears to be less consistent, possibly attributed to insufficient training data. This observation aligns logically with the fact that asphalt roads constitute a significant portion of the point cloud data, resulting in a larger pool of training data compared to other categories.

Conclusion

In conclusion, PointNet++ demonstrates effectiveness when sufficient training data is available, leading to accurate results. However, it does have certain limitations. Achieving a 95% accuracy level necessitates a substantial amount of training data. Additionally, the program only supports training in a single session and lacks the capability to incrementally train a new model based on an

existing one with a new dataset. Given the reliance on extensive data, this limitation can pose challenges.

For future enhancements, it is recommended that the program be updated to allow users to train a new model based on the progress of the old model with new datasets. Another potential improvement involves tailoring the deep learning model to better suit road environments, aiming to deliver accurate results with a reduced dependency on extensive training data.

Bibliography

- Duffell, C. G., and D. M. Rudrum. (2005). Remote sensing techniques for highway earthworks assessment. *Site Characterization and Modeling*. 2005. 1-13.
- Gargoum, S., & El-Basyouny, K. (2019). Effects of LiDAR point density on extraction of traffic signs: A sensitivity study. *Transportation Research Record*, 2673(1), 41-51.
- Garzón Barrero, J., Cubides Burbano, C. E., & Jiménez-Cleves, G. (2021). Quantifying the effect of LiDAR data density on DEM quality. *Ciencia e Ingeniería Neogranadina*, 31(2), 149-169.
- Ghallabi, F., El-Haj-Shhade, G., Mittet, M. A., & Nashashibi, F. (2019, June). LIDAR-based road signs detection for vehicle localization in an HD map. In *2019 IEEE Intelligent Vehicles Symposium (IV)*, 1484-1490.
- Hu, Y. (2003). Automated extraction of digital terrain models, roads and buildings using airborne LiDAR data (pp. 85-88). University of Calgary, Department of Geomatics Engineering.
- Javanmardi, M., Song, Z., & Qi, X. (2019). Automated traffic sign and light pole detection in mobile LiDAR scanning data. *IET Intelligent Transport Systems*, 13(5), 803-815.
- Williams, K., Olsen, M. J., Roe, G. V., & Glennie, C. (2013). Synthesis of transportation applications of mobile LiDAR. *Remote Sensing*, 5(9), 4652-4692.
- Wu, S., Wen, C., Luo, H., Chen, Y., Wang, C., & Li, J. (2015, July). Using mobile LiDAR point clouds for traffic sign detection and sign visibility estimation. In *2015 IEEE International Geoscience and Remote Sensing Symposium (IGARSS)*, 565-568.
- Yen, K. S., Ravani, B., & Lasky, T. A. (2011). LiDAR for data efficiency (No. WA-RD 778.1). Washington (State). Dept. of Transportation. Office of Research and Library Services. <https://www.wsdot.wa.gov/research/reports/fullreports/778.1.pdf>
- Yu, Y., Li, J., Guan, H., & Wang, C. (2014, July). 3D crack skeleton extraction from mobile LiDAR point clouds. In *2014 IEEE Geoscience and Remote Sensing Symposium*, 914-917.
- Zhang, S., Wang, C., Lin, L., Wen, C., Yang, C., Zhang, Z., & Li, J. (2019). Automated visual recognizability evaluation of traffic sign based on 3D LiDAR point clouds. *Remote Sensing*, 11(12), 1453.

Dataset Citation: 2014 USGS QL 2 LiDAR: San Diego, CA Point Cloud files with
Orthometric Vertical Datum North American Vertical Datum of 1988 (NAVD88) using
GEOID18 distributed by OpenTopography
[<https://portal.opentopography.org/noaaDataset?noaaID=8611>] Accessed: 2023-12-19,
Use License: CC BY 4.0

About the Authors

Yushin Ahn

Dr. Yushin Ahn is an associate professor in the Department of Civil and Geomatics Engineering, California State University at Fresno, CA. He received his B. Eng. degree in Civil Engineering and his M.Sc. degree in surveying and digital photogrammetry from Inha University, Korea, in 1998 and 2000, respectively, and his M.Sc. and Ph.D. degrees in Geodetic Science from Ohio State University, Columbus, in 2005 and 2008, respectively. His research interests include digital photogrammetry, feature tracking, and sensor calibration and integration. Dr. Ahn received the Robert E. Altenhofen Memorial Scholarship from the American Society for Photogrammetry and Remote Sensing. He has been a certified photogrammetrist since 2014.

Riadh Munjy

Dr. Riadh Munjy got his B.S. in Civil Engineering in 1978 from the University of Baghdad, Iraq, an MSCE in Civil Engineering in 1979, an MS in Applied Mathematics in 1981, and a Ph.D. in Civil Engineering in 1982 from the University of Washington. He has been a faculty member and an active researcher at California University, Fresno since 1982 and has been a Professor of Civil and Geomatics Engineering since 1988 and the chair of the Civil and Geomatics Engineering Department since 2014. He has over forty years of experience in teaching courses in photogrammetry, digital mapping, GIS, and least squares adjustment. In 1997, he was awarded the Meritorious Service Award by ASPRS. He has also been awarded the Fairchild Photogrammetric Award (2014), the 2020 Fellow Award, and the 2023 Lifetime Achievement Award.

Ziyuan Li

Ziyuan Li is a senior undergraduate pursuing a B.A. in Electrical Engineering at California State University, Fresno. He has two years of research experience in the power electronics field. He is also familiar with tools such as MATLAB and Simulink.

Hon. Norman Y. Mineta

MTI BOARD OF TRUSTEES

Founder, Honorable Norman Mineta***
Secretary (ret.),
US Department of Transportation

**Chair,
Jeff Morales**
Managing Principal
InfraStrategies, LLC

**Vice Chair,
Donna DeMartino**
Retired Transportation Executive

**Executive Director,
Karen Philbrick, PhD***
Mineta Transportation Institute
San José State University

Rashidi Barnes
CEO
Tri Delta Transit

David Castagnetti
Partner
Dentons Global Advisors

Maria Cino
Vice President
America & U.S. Government
Relations Hewlett-Packard Enterprise

Grace Crunican**
Owner
Crunican LLC

John Flaherty
Senior Fellow
Silicon Valley American
Leadership Forum

Stephen J. Gardner*
President & CEO
Amtrak

Ian Jefferies*
President & CEO
Association of American Railroads

Diane Woodend Jones
Principal & Chair of Board
Lea + Elliott, Inc.

Priya Kannan, PhD*
Dean
Lucas College and
Graduate School of Business
San José State University

Will Kempton**
Retired Transportation Executive

David S. Kim
Senior Vice President
Principal, National Transportation
Policy and Multimodal Strategy
WSP

Therese McMillan
Retired Executive Director
Metropolitan Transportation
Commission (MTC)

Abbas Mohaddes
CEO
Econolite Group Inc.

Stephen Morrissey
Vice President – Regulatory and
Policy
United Airlines

Toks Omishakin*
Secretary
California State Transportation
Agency (CALSTA)

April Rai
President & CEO
Conference of Minority
Transportation Officials (COMTO)

Greg Regan*
President
Transportation Trades Department,
AFL-CIO

Rodney Slater
Partner
Squire Patton Boggs

Paul Skoutelas*
President & CEO
American Public Transportation
Association (APTA)

Kimberly Slaughter
CEO
Sysra USA

Tony Tavares*
Director
California Department of
Transportation (Caltrans)

Jim Tymon*
Executive Director
American Association of
State Highway and Transportation
Officials (AASHTO)

Josue Vaglienty
Senior Program Manager
Orange County Transportation
Authority (OCTA)

* = Ex-Officio
** = Past Chair, Board of Trustees
*** = Deceased

Directors

Karen Philbrick, PhD
Executive Director

Hilary Nixon, PhD
Deputy Executive Director

Asha Weinstein Agrawal, PhD
Education Director
National Transportation Finance
Center Director

Brian Michael Jenkins
National Transportation Security
Center Director

